Journal of Hydrology 608 (2022) 127772

Contents lists available at ScienceDirect

Journal of Hydrology

journal homepage: www.elsevier.com/locate/jhydrol

Research papers

Storm event analysis of four forested catchments on the Atlantic coastal plain using a modified SCS-CN rainfall-runoff model

D.M. Amatya[a,*], A. Walega[b], T.J. Callahan[c], A. Morrison[d,1], V. Vulava[c], D.R. Hitchcock[e], T. M. Williams[e], T. Epps[f]

[a] USDA Forest Service, Center for Forest Watershed Science, 3734 Highway 402, Cordesville, SC 29434, USA
[b] Department of Sanitary Engineering and Water Management, University of Agriculture in Krakow, Krakow, Mickiewicza Street 24/28, 30-059 Krakow, Poland
[c] Department of Geology and Environmental Geosciences, College of Charleston, 66 George Street, Charleston, SC 29424, USA
[d] Environmental and Sustainability Studies Program, College of Charleston, 66 George Street, Charleston, SC USA
[e] Department of Agricultural Sciences, Baruch Institute of Coastal Ecology and Forest Science, Clemson University, P.O. Box 596, Georgetown, SC, USA
[f] Craftwater Engineering, Portland, OR, USA

ARTICLE INFO

This manuscript was handled by Marco Borga, Editor-in-Chief, with the assistance of Massimiliano Zappa, Associate Editor

Keywords:
Overland surface runoff
Shallow subsurface saturated runoff
Water table
Antecedent soil moisture
Poorly drained soils

ABSTRACT

In this study, we calibrated and tested the Soil Conservation Service Curve Number (SCS-CN) based Modified Sahu-Mishra-Eldo (MSME) model for predicting storm event direct runoff (Q_{tot}) and its soil saturation coefficient α as a threshold antecedent moisture condition for partitioning into overland surface and shallow subsurface runoff components. The model calibration was performed using 36 storm events from 2008 to 2015 on a 160-ha low-gradient forested watershed (WS80) on poorly drained soil. The model was further validated without calibration using data from 2011 to 2015 on two sites [115 ha (Conifer) and 210 ha (Eccles Church)] and from 2008 to 2011 on a third site, the 100-ha Upper Debidue Creek (UDC), all similar forested watersheds on the Atlantic Coastal Plain, USA. The calibrated MSME model was able to accurately predict the estimated $Q_{tot\,pred}$ for the WS80 watershed, with calculated Nash-Sutcliffe efficiency coefficient (NSE), RMSE-standard deviation ratio (RSR), and percent bias (PBIAS) of 0.80, 0.44, and 16.7%, respectively. By applying the same calibrated α value of 0.639 from the WS80 to two other similar poorly drained watersheds, the MSME model satisfactorily predicted the estimated $Q_{tot\,pred}$ for both the Eccles Church (NSE = 0.64; RSR = 0.57; PBIAS = 28.9%) and Conifer (NSE = 0.60; RSR = 0.58; PBIAS = 21.3%) watersheds, respectively. The MSME model, however, yielded unsatisfactory results (NSE = -0.13, RSR = 2.06, PBIAS = 616.3%) on the UDC watershed with coarse-textured soils, indicating the possible association of the α coefficient with soil subsurface texture. Based on the analysis of event rainfall and pre-event water table elevation, and linking them with the calibrated α coefficient that describes the proportion of saturated depth in a soil profile, it was found that rainfall was the main determining factor for overland runoff generation. These results demonstrate the MSME model's potential to predict direct runoff in poorly drained forested watersheds, which serve as a reference for urbanizing coastal landscapes in a changing climate.

1. Introduction

Runoff and streamflow processes in topographically low-gradient coastal watersheds are dominated by shallow subsurface drainage from saturated areas and saturation excess overland surface runoff that occurs when a shallow water table (WT) is present (Amatya et al., 2019; Epps et al., 2013a; Slattery et al., 2006). These low-gradient watershed areas, generally located along the Atlantic and Gulf Coastal plain regions in the U.S., are rapidly being developed and urbanized.

Baseline reference data on storm runoff characteristics of unimpaired watersheds are crucial for describing and assessing the hydrological impacts of developing areas and urbanization in these and other similar coastal watersheds.

A number of studies have attempted to describe such storm event characteristics using data for headwater coastal watersheds in the southeastern Atlantic coastal plain (Amatya et al., 2000; 2019; Blair

* Corresponding author.
E-mail address: devendra.m.amatya@usda.gov (D.M. Amatya).
[1] Now at: Southface Institute, 241 Pine Street NE, Atlanta, GA, USA.

https://doi.org/10.1016/j.jhydrol.2022.127772
Received 4 June 2021; Received in revised form 15 March 2022; Accepted 25 March 2022
Available online 31 March 2022
0022-1694/Published by Elsevier B.V.

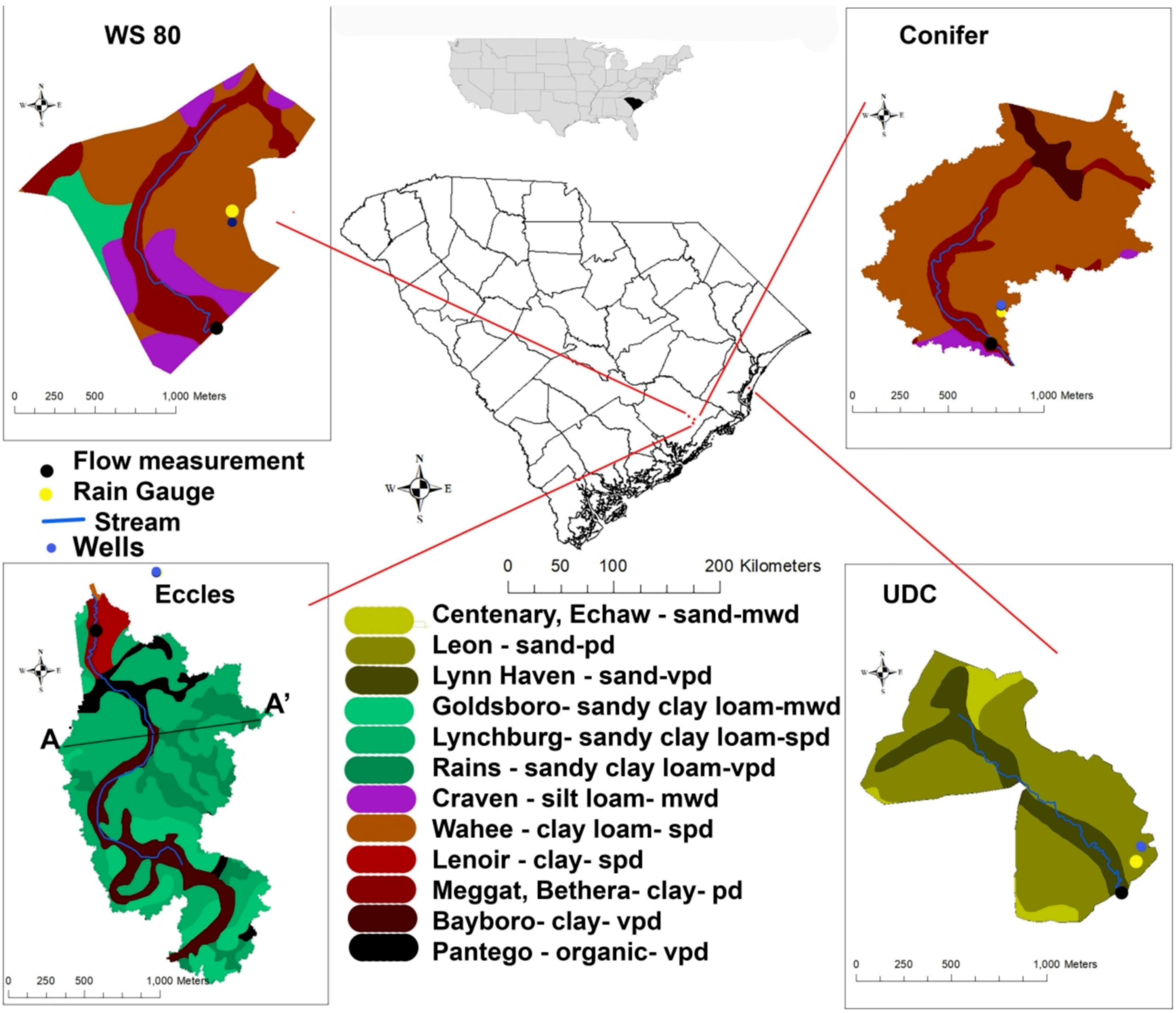

Fig. 1. Location and soil distribution maps for WS80, Conifer, Eccles Church, and UDC watersheds with their wells, rain gauges, and flow gauging stations. Listed for each soil is the soil series name, subsurface soil texture, and soil drainage class (*mwd*-moderately well drained, *spd*- somewhat poorly drained, *pd*- poorly drained, *vpd*-very poorly drained). Note line A-A' is used in Fig. 9 below.

et al., 2014; Bosch et al., 2017; Capece et al., 1986; Epps et al., 2013a; La Torre Torres et al., 2011; Sheridan et al., 2002; Swindel et al., 1983), a region characterized by a low-gradient forested landscape that is undergoing significant residential and commercial development (O'Driscoll et al., 2010; Hitchcock et al., 2014; Lockaby et al., 2013). At the same time, multiple hydrologic models of varying complexities and scales have been used to estimate/predict runoff response to storm events from catchments with various topographic and land cover conditions (Blair et al., 2014; Fedelman, 2000; Genereux, 2003; Hayes and Young, 2006; Kannan et al., 2007; Rossman and Huber, 2016; USDA, 2004). For example, the Rational Method (Kuichling, 1889), the Soil Conservation Service (SCS) Curve Number (*CN*) method (USDA 2004), and HEC-HMS (HEC, 2006; Menberu et al., 2014) model serve as some examples, among others. There are several studies in the literature on the modification of the original SCS-CN method to assess direct runoff (Blair et al., 2014; Epps et al., 2013a; Grimaldi et al., 2013a; 2013b; Kannan et al., 2007; Młyński et al., 2020; Verma et al., 2020). However, uncertainty remains due to a large range of estimates of runoff volume and peak flow response to storm events obtained from these models (Genereux, 2003; Joo et al., 2014; Walega et al., 2020). Only a limited number of such models have been tested on forest systems (Corbin et al., 2022; Tedela et al., 2012), particularly on less studied small low-gradient watersheds.

Some of the recently modified versions of the SCS-CN models (Bartlett et al., 2016; Blair et al., 2012; Walega et al., 2020) have shown improvement in predictions of storm response on relatively undisturbed headwater forested watersheds, thus informing better stormwater management in such landscapes that are undergoing development. For example, stormflow on lower coastal plain (LCP) watersheds was shown to be driven by the WT depth and antecedent soil moisture (ASM); stormflow increases substantially as shallow overland surface runoff soon after near-surface saturation or surface ponding (Epps et al., 2013a; Harder et al., 2007; Slattery et al., 2006). Epps et al. (2013b) showed that event runoff predictions do not compare closely to measured flow under the average moisture condition normally associated with the SCS-CN method (USDA, 2004), warranting adjustments of the *CN* for WT-based ASM. Most of these studies applied the standard SCS-CN model, but with a modified initial abstraction component to predict direct runoff for the shallow WT conditions in this region (Blair et al., 2014; Epps et al., 2013b; La Torre Torres, 2008). Blair et al. (2012) developed and successfully tested the SWARM model to predict runoff volume and peak discharge with limited data for some LCP watersheds of South

Table 1
Characteristics of study watersheds (WS80, Conifer, Eccles Church, and UDC).

Study Site	WS80	Conifer	Eccles Church	UDC
Latitude, degrees	33.15 79.8° W	33.12	33.11	33.39
Longitude, degrees	−79.80	−79.74	−79.76	−79.17
Elevation range, m	3.5–10.0	6.9–10.6	7.39 – 11.5	1.8 – 6.5
Average basin slope, %	< 2.0	0.23	0.14	< 1.0
Area, ha	160	115	210	110
Channel Slope, %	0.22	0.22	0.10	0.21
Maximum Channel length, m	2020	1300	2780	1740
Basin Shape Factor[a]	1.19	0.13	0.43	1.94
Weighted average CN	67	78	77	55
Dominant soil type[b]	Wahee	Wahee/ Lenoir	Lynchburg	Leon/Lynn Haven
HSG of dominant soil type[c]	D	C/D	B/D	A/D
Dominant vegetation type	Pine mixed hardwood	Pine (45%)	Pine (39%)	Pine
Dominant land use type	Unmanaged	Dense (84%)	Thinned (57%)	Unmanaged
Forested wetlands (%)	48	10.5	20.0	83

[a] Basin shape factor is the square of the length of the longest flow path in a stream basin divided by the drainage area.
[b] Wahee soil series: fine, mixed, semiactive, thermic Aeric Endoaquults.
Lynchburg soil series: fine-loamy, siliceous, semiactive, thermic Aeric Paleaquults.
Lenoir soil series: fine, mixed, semiactive, thermic Aeric Paleaquults.
Leon soil series: sandy, siliceous, thermic Aeric Alaquods.
Lynn Haven soil series: sandy, siliceous, thermic Typic Alaquods.
[c] HSG: hydrologic soil group.

Carolina. Bartlett et al. (2016) moved beyond the classic SCS-CN by accommodating different runoff concepts and distributions of heterogeneities in storage capacity and soil moisture as the basis for upscaling a point runoff response and linking ecohydrological processes to runoff modeling. Those authors showed proof of concept in four forested watersheds and argued that their resulting model may better represent geographic regions and site types that previously have been beyond the scope of the traditional SCS-CN method. However, all those watersheds were on upland sites where hillslope hydrology dominates runoff generation (Hewlett, 1982). A recent previous version of the modified SCS-CN (SME_m), which includes a single modified ASM, was found to perform better than the SCS-CN model, but still relatively unsatisfactory in predicting total direct runoff and peak discharge on a low-gradient coastal forest watershed (Walega et al., 2020).

Most recently, building on the SME_m model (Walega et al., 2020), the MSME (Modified Sahu-Mishra-Eldho) model was developed, which incorporates a soil saturation coefficient α for partitioning the total direct runoff into the overland surface and saturated subsurface runoff based on the ASM with the WT as a proxy. This is somewhat similar to the concept in Bartlett et al. (2016) to more accurately predict storm response to event outflow and peak discharge rates. The model was successfully tested for predicting $Q_{tot\,pred}$ in an artificially drained coastal forested watershed with open ditches 100 m apart (Walega and Amatya, 2020). Results showed computed $Q_{tot\,pred}$ was completely dominated by saturated subsurface runoff (as drainage in the ditch) driven by the gradient between the WT midway between the ditches and ditch water level with negligible overland surface runoff, consistent with earlier studies (Amatya et al., 1996; Skaggs et al., 2016). However, to date, the MSME model has not been tested in naturally drained (no ditch system) forest watersheds, where both forms of direct runoff are possible to occur. Amatya et al. (2019) reported that on low-gradient watersheds lateral subsurface flow and soil moisture storage vary widely with the balance of rainfall and evapotranspiration (ET), with lateral flow likely occurring for only a short distance, about 50–100 m as in the case of ditched systems.

Without drainage or with a low drainage density in low-gradient watersheds, the shallow WT position during dry periods would be near the stream channel bottoms. During a storm event, only a small amount of rainwater is needed to cause a rapid rise in the WT, resulting in a larger hydraulic gradient and thus causing subsurface flow towards the stream (Bonnel, 1993). During wet periods, WT rise results in near-surface lateral subsurface flow, which redistributes water to compensate for ET and microtopographic variation (Younger, 2006). Such a process is described as subsurface stormflow common in humid climatic regions (Slattery et al., 2006). As the WT approaches the surface in a broad inter-stream area, watershedwide overland surface runoff occurs depending upon the microtopography. Once the groundwater is recharged and the WT has risen to the surface, precipitation to these areas will become runoff, regardless of rainfall intensity, and water travels quickly to the stream (Dingman, 2002). Conceptually different from the classical concepts developed by Hewlett (1982) for upland hillslope hydrology, in which subsurface stormflow is defined as "interflow" and surface stormflow as "overland runoff, the process of saturation excess runoff generation is common in humid, low-gradient systems with a shallow WT (Slattery et al., 2006; Younger, 2006). The concept of direct runoff and its components (saturated subsurface interpreted as "streamside" drainage and overland surface runoff interpreted as "watershedwide" runoff) on low-gradient forest systems, primarily affected by soil moisture with the WT as a proxy, were implemented in the MSME model as an advancement in the SCS-CN method applicable to areas<300 ha, typically with less spatial variability in the soil moisture deficit (Famiglietti et al., 2008, as cited in Bartlett et al. 2016).

In this study, we applied the MSME model on four first-order catchments in naturally drained low-gradient forests on the South Carolina Atlantic Coastal Plain to examine rainfall-runoff processes as influenced by the antecedent moisture condition (AMC). We used measured storm event data from 2008 to 2015 for the one watershed (160 ha), data from 2011 to 2015 for two watersheds (110 ha and 210 ha), and data from 2008 to 2011 for a fourth watershed (100 ha) (Fig. 1). The main objectives of this study were (1) to calibrate the MSME model for the WS80 watershed, and (2) to validate its performance by predicting observed storm event direct runoff $Q_{tot\,obs}$ for the three remaining watersheds without any calibration. The hypotheses tested were:

1) The MSME model using the published SCS-CN values and calibrated with storm event data for other parameters on the poorly drained WS80 watershed can accurately predict the observed storm event-based total direct runoff $Q_{tot\,obs}$ based on accepted statistical criteria.
2) There exists a threshold for both the pre-event initial water table elevation (WTE) and precipitation amount, identified using the calibrated soil saturation coefficient α, above which event overland surface runoff is predicted, in addition to predicted subsurface saturated runoff on this watershed.

2. Material and methods

2.1. Study site description

Four first-order watersheds were studied: WS80 (1.60 km^2), Eccles Church (2.10 km^2), Conifer (1.15 km^2), and Upper Debidue Creek (UDC) (1.00 km^2). The hydrologic unit code (HUC) for the first three watersheds is 0305020103, and the HUC for UDC is 0302040804. The Eccles Church and Conifer watersheds are within the third-order Turkey Creek

(TC) watershed (52.4 km^2) (Fig. 1) in the USDA Forest Service Francis Marion National Forest (FMNF), located approximately 60 km northeast of Charleston, South Carolina (Morrison, 2016).

The WS80, Conifer, and Eccles Church watersheds [within the larger Turkey Creek (TC) watershed] are rural, forested lands, that drain to Turkey Creek, which discharges to Huger Creek, a headwater catchment of the East Branch of the Cooper River. That catchment ultimately drains into the Charleston Harbor (Harder et al., 2007; James, 2013; La Torre Torres et al., 2011). Separately, the UDC watershed (located in coastal Georgetown County, South Carolina) is part of the freshwater portion of Debidue Creek in the North Inlet estuary (Epps et al., 2013a). UDC drains into an area with an existing suburban housing development and then into the North Inlet tidal saltwater estuary. All four watersheds are characterized by low-gradient topography and shallow water table conditions. Long-term (1946–2008) average annual minimum and maximum air temperatures were 3.2 and 30.6 °C, respectively, and the annual rainfall ranged from 834 to 2106 mm on the USFS Santee Experimental Forest (SEF) site. July and November were, on average, the wettest (187 mm mean rainfall) and the driest (69 mm mean rainfall) months, respectively (Dai et al., 2013).

The WS80 watershed is on the north bank of Turkey Creek and is the control catchment of a paired system. The watershed is comprised of about 70% mixed pine and hardwood stands and 48% forested wetland based on the U.S. National Wetlands Inventory classification (NWI, 2021). WS80 has poorly drained soils, primarily of the Wahee soil series (fine, mixed, semiactive, thermic Aeric Endoaquults), which has a large field capacity and small permeability (Harder et al., 2007). The Eccles Church watershed is located on the south bank of the TC watershed. The dominant vegetation of the Eccles Church watershed is loblolly pine (*Pinus taeda*), followed by longleaf pine (*Pinus palustris*) (Table 1); the dominant land use is thinned forest (basal area < 25 m^2 ha^{-1}), followed by dense forest (basal area > 25 m^2 ha^{-1}), and the dominant soil series are Lynchburg (48.6%) and Goldsboro (14%) (Morrison, 2016). The Conifer watershed is located on the right (north) bank of the TC watershed. Loblolly pine is the dominant land cover followed by the longleaf pine. Land use is dense forest and the primary soil series is Wahee/Lenoir (79%). Other watershed characteristics are presented in Table 1 with more details in Morrison (2016).

The UDC watershed is characterized by low-gradient topography and shallow water table conditions (Epps et al. 2013a). The landscape is currently forested with mixed hardwood lowlands and upland pine stands. Based on the National Land Cover Database (NLCD, 2016), the watershed is comprised of 83% vegetated wetland, much higher than the other three watersheds in this study. The primary soil series in the UDC watershed are Lynn Haven and Leon. These soils are formed in sandy marine sediments and are associated with very low-gradient conditions, high permeability, and are poorly to very poorly drained (USDA, 1980).

2.2. Data collection

Rainfall data for the Eccles Church and Conifer watersheds were collected at a weather station approximately 3 km east of the study sites (Fig. 1). An automatic tipping bucket rain gauge with an adjacent manual gauge was used. Rainfall for both WS80 and UDC watersheds were also collected using an automatic tipping bucket backed up by a manual gauge (Fig. 1). Additional rain gauges approximately 6 km west at the Turkey Creek outlet (USGS gauge) and at the SEF were used to fill data gaps on WS80, Eccles, and Conifer watersheds.

Flow rates were estimated by the standard culvert area-velocity method using stage and corresponding velocity data collected at 15-min intervals using an automated ISCO 4150 flow meter (Teledyne™, Inc., Thousand Oaks, CA, USA) installed inside and at the downstream end of round concrete culverts that were 914 mm and 762 mm in diameter for the Eccles Church and Conifer watersheds, respectively. Flow rates for 15-min intervals were integrated to compute stream discharge (volumetric flow) and to estimate event-based total streamflow (i.e., outflow) (Morrison, 2016). Digital measurements of stage recorded every 10-minutes by a Teledyne ISCO flowmeter installed upstream of the WS80 watershed weir outlet gauging stations were used with established rating curves for compound V-notch weir for estimating streamflow rates (Amatya and Trettin, 2019; 2021). Watershed outflow rate in the UDC was estimated using a 0.6-m modified Parshall flume located immediately downstream of a road culvert (Epps et al., 2013a; Hitchcock et al., 2009).

Shallow groundwater data (i.e. depth to water table from ground surface) were measured on an hourly basis using a Global Water WL-16 pressure transducer (Xylem™, Inc., Rye Brook, NY, USA) with a data-logger on an upland well on WS80 (Amatya and Trettin, 2021) and in the wells on Lynchburg and Wahee soils near the Eccles Church and Conifer watersheds, respectively (Amatya et al., 2018; Morrison, 2016). A water table well with a pressure transducer/Solinist™ logger (Georgetown, Ontario, Canada) was located in an upland pine area near the UDC watershed boundary (Epps et al., 2013a). Additional details of hydro-meteorological measurements may be found elsewhere (Amatya and Trettin, 2021; Epps et al., 2013a; Morrison, 2016).

2.3. Hydrograph separation

Separation of storm event hydrographs into direct runoff and base-flow values for all watersheds were conducted primarily following techniques used by Williams (2007), as cited in Epps et al. (2013a), in which a log-linear regression line was fit for the exponential receding limb of the hydrographs for the UDC and WS80. However, a linear regression with the same separation technique was used by Morrison (2016) for Eccles and Conifer watersheds. Storm events were selected using rainfall and streamflow data during 2008–2015 for WS80, 2008–2011 for UDC, and 2011–2015 period for the Eccles Church and Conifer watersheds. Individual storm events were selected for each of the watersheds and flow rate data were plotted against the corresponding rainfall that may have triggered the event. Two screening criteria were selected to identify storm events: 1) events with a single-peak hydrograph and 2) event rainfall of at least 12 mm and minimum of six hours between rainfall events (Amatya et al. 2000; Epps et al. 2013a; La Torres et al. 2011), although all events exceeded 20 mm size, except for two events on the Eccles Church watershed. Events with a small double peak were also analyzed for comparison. Storm event outflow characteristics evaluated included total stream outflow (mm), and direct runoff (Q_{tot_obs}) which was calculated as a difference between total outflow and baseflow obtained using hydrograph separation (Epps et al., 2013a; Morrison, 2016). Total 5-day rainfall (*P5*) amount before the start of each event was also tabulated as proxies for the ASM. Out of the 36 events analyzed for the WS80 watershed, 20 events occurred during the winter and spring seasons (November to April), with smaller ET demand, and 16 events were during the summer and fall seasons (May to October) with larger ET. The WT data from the wells in Wahee soil on the WS80 watershed (Amatya and Trettin, 2021), in the dominant Wahee/Lenoir soil on Conifer, in the Lynchburg soil for Eccles Church (Morrison, 2016), and Leon soils on the UDC (Epps et al., 2013a) watersheds were used in the analysis. All of these wells, installed in different soil series with varying soil drainage and infiltration response, also provided information on water table position, as a surrogate for ASM conditions, for the area (Amatya and Trettin, 2010; Amatya et al., 2018; Callahan et al., 2012; Epps et al., 2013a; Williams and Amatya, 2016; Zhai et al., 2020).

2.4. SCS-CN Model and Modified Sahu-Mishra-Eldho (MSME) model

Direct runoff (Q_{tot_pred}) for all events on all four watersheds was predicted using the MSME model. The model was also used to simulate both the subsurface saturated "streamside" (Q_{subs_pred}) and shallow "watershedwide" surface overland runoff (Q_{surf_pred}) components of the direct runoff (Q_{tot_pred}). Saturated groundwater flow, in the form of

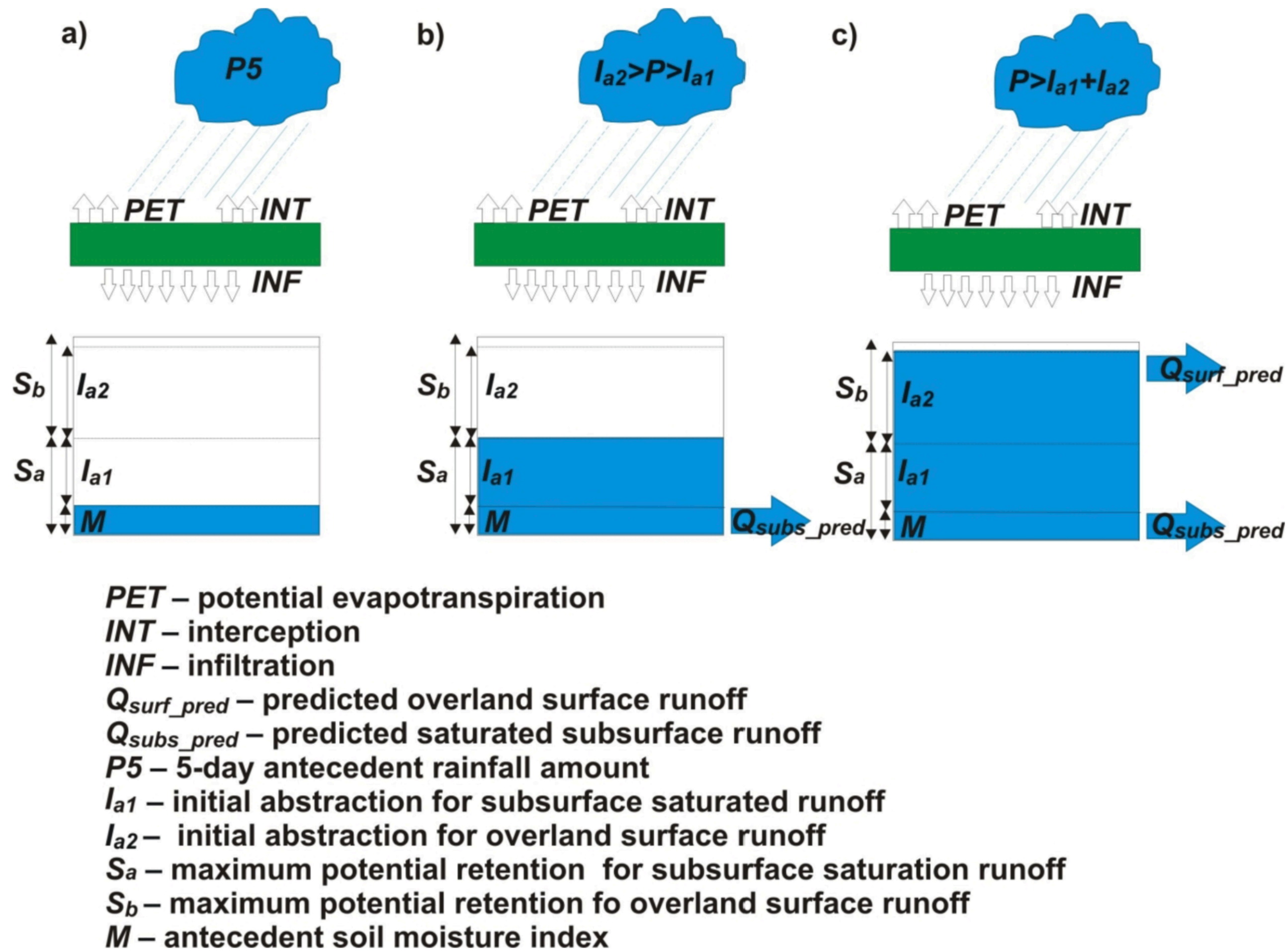

Fig. 2. A conceptual diagram of components of direct runoff formation in the MSME model.

baseflow to receiving waters, is not considered in the MSME model. The model functions somewhat similar to '*ab*' components of the '*abcd*' conceptual model formulated for upper and lower zone soil moisture as cited in Martinez and Gupta (2011), to predict only (1-*c*) as direct runoff, and not '*d*' for the baseflow.

2.4.1. Theoretical background of the runoff formation in the MSME model

In the MSME model, it is assumed that in the initial phase of rainfall, when the soil has antecedent moisture *M* after *P5*, direct runoff does not occur (Fig. 2a). The *M* is determined by infiltrated water from *P5*, after exceeding the interception, depression storage and potential evapotranspiration *(PET)* losses. Past studies (Blair et al., 2014; Baltas 2007; Hawkins et al., 2002; Mishra and Singh, 2002; Soulis and Valiantzas, 2012; Woodward et al. 2003) have reported that the initial abstraction, I_a, was overestimated when calculated using the original method. In this model, we used the *M* parameter to reduce I_a compared to the original method (Appendix A), which seems to be more relevant on low-gradient watersheds with high water table elevation. During a storm event, when the sum of precipitation *P* exceeds the first soil saturation threshold *Ia1*, subsurface stormflow begins (Fig. 2b). If the rainfall *P* continues during the event, the soil profile will continue to be saturated, achieving the second threshold (I_{a2}), resulting in the occurrence of overland surface runoff (Fig. 2c). The I_{a1} and I_{a2} parameters are determined not only by *M* and but also by the saturated area of the watershed.

At the beginning of rainfall only a small part of the watershed, mainly located close to the stream, can be saturated because the land surface WTE is relatively deeper to be hydraulically connected with the stream water level. During longer duration storms, the saturated area tends to increase widely across many more parts of the watershed, potentially generating saturated surface stormflow. The factor determining the proportion of saturated areas in the whole watershed is the soil saturation parameter α. We hypothesized that the soil profile in the watershed is completely saturated when $\alpha = 1.0$. If the soil profile is only partially saturated ($\alpha < 1.0$), storm subsurface runoff may occur only from the part of the watershed located closest to the water course.

This α coefficient in the MSME represents the saturation in the soil column, similar to the '*b*' as water holding capacity of upper soil zone conceptualized in the '*abcd*' model cited in Martinez and Gupta (2011) where direct runoff '(1-*c*)' depends upon the soil available moisture after subtracting recharge (*c*) for baseflow. Interestingly, the '*a*' parameter in the '*abcd*' model represents the runoff propensity index similar to the threshold for generating the Q_{surf} as will be discussed below. The key difference is that the MSME model further attempts to partition direct runoff '(1-*c*)' into Q_{subs_pred} and Q_{surf_pred}, which were calculated by introducing different soil moisture conditions expressed by S_a, S_b, and two thresholds of initial abstractions, I_{a1} and I_{a2}. Both the initial abstractions are linked with the α coefficient. In addition, the I_a, which relies on interception, surface storage, and infiltration, is also adjusted by the soil moisture *M* as an index parameter in the model, with increased *M* primarily reducing initial abstraction I_a. The coefficient α obtained by calibration for the proportion of saturated soil in the profile plays a significant role in identifying a threshold of WTE while transitioning from Q_{subs_pred} to Q_{surf_pred}. This is similar to Bartlett et al. (2016) who used antecedent soil moisture deficit '*c*' in their model like the α coefficient in the MSME model. In both cases, these coefficients represent soil moisture conditions before rainfall events. However, the MSME

Table 2
Statistical characteristics of selected rainfall-runoff events (N = 36) from the 2008–2015 period, MSME model parameters, and predicted event runoff components for the WS80 watershed.

Parameter	*P*	*P5*	Q_{tot_obs}	*CN*	*M*	S_a	S_b	I_{a1}	I_{a2}	Q_{surf_pred}	Q_{subs_pred}	Q_{tot_pred}
	mm	mm	mm		mm	mm	mm	mm	mm	mm	mm	mm
Mean	73.1	19.3	13.2	66.7	3.6	86.5	220.4	53	79.6	0.5	10.6	11
Median	66.5	12	9.8	66	0	88.3	198.3	43.1	71.6	0	3.8	3.8
Minimum	29	0	0	57	0	22.1	121.5	9.5	43.9	0	0	0
Maximum	157.7	147	88	88	41.5	122.4	672.4	78.2	242.7	8.1	82.2	83.6
Standard dev.	32.7	29.2	16.1	10.3	8.8	37.2	134.4	23.9	48.5	1.6	15.8	16.5
COV	0.4	1.5	1.2	0.2	2.5	0.4	0.6	0.5	0.6	3.4	1.5	1.5
Kurtosis	1	11	12.8	−1.3	11.3	−1.8	5.6	−1.7	5.6	17.5	11.5	9.9
Skewness	1.1	3.1	3	0.3	3.3	−0.1	2.1	−0.1	2.1	4	2.9	2.7

P: sum of the event precipitation, *P5*: 5-day antecedent rainfall amount, Q_{tot_obs}: observed total direct runoff, *CN*: calculated curve number. *M*: antecedent soil moisture index, S_a: maximum potential retention for the area where subsurface saturated runoff occurs, I_{a1}: initial abstraction for subsurface saturated runoff, I_{a2}: initial abstraction for overland surface runoff (mm), S_b: maximum potential retention for the area where overland runoff occurs (mm), Q_{surf_pred} – predicted overland surface runoff, Q_{subs_pred} – predicted subsurface saturated runoff, Q_{tot_pred} predicted total runoff.

Table 3
Parameters of the MSME model and measures of goodness-of-fit statistics for predicting the total surface runoff on all watersheds.

Watershed	α	λ	β	PBIAS, %	RSR	NSE
WS80	0.639	0.268	0.703	16.70	0.44	0.80
Eccles	0.639	0.268	0.703	28.93	0.57	0.64
Conifer	0.639	0.268	0.703	21.34	0.58	0.60
UDC	0.639	0.268	0.703	616.29	2.06	−0.13

* Coefficient and parameters of the model on Eccles Church, Conifer, and UDC watersheds, were assumed the same as on the WS80 watershed.

Table 4
Comparison of computed statistical criteria used for the analysis of simulated conditions for all events.

Uncertainty parameter	Value of parameters
ARIL	0.496
AAD	0.797
ADA, mm	11.32
P-95 CI, %	44.44

model is a lumped model with parameters describing antecedent moisture representative of the soil profile in a small homogenous area where the SCS-CN is applicable, in contrast with the Bartlett et al. (2016) who modified the SCS-CN method allowing to capture runoff from small rainfall events that do not activate large areas of threshold-excess runoff and, thus, better represent various geographic regions and site types. The later model using probabilistic distributions to consider heterogeneities in rainfall and soil water storage distribution was shown to perform better than the SCS-CN model on upland watersheds.

The potential water retention parameters, *Sa* and *Sb,* were calculated based on the same approach as in the original SCS-CN method where CN is a critical parameter. The CN value was obtained from the published NRCS tables (USDA 2004) using the land cover/conditions and soil hydrologic group for each area covered by a soil type within a watershed. Then an area-weighted average CN (for AMCII) was calculated and presented in Table 1 for each of the watersheds (Haley, 2007; Epps et al., 2013b). In the MSME model for this study, the weighted CN in Table 1 was further modified for different antecedent moisture conditions for each of the storm events, producing different weighted CNs with their calculated statistics shown in Table 2.

Each of the CN values in Tables 2, 5, 6, and 7 used in the MSME model for the four watersheds, was obtained as a storm-event average of the weighted CN-II (Table 1) modified for antecedent moisture conditions (AMC) (dry- AMCI, wet-AMCIII, and average AMC-II) for each of the storm events. The observed rainfall-runoff data were plotted against calculated runoff for each rainfall based on the SCS-CN method where CN was assumed for AMCI, AMCII and AMCIII. An example of this is presented in Fig B1 for watershed WS80. Next, each observed runoff was compared to theoretical line of direct runoff for each of the three AMC values, and the final CN value in the MSME model was based on distance between observed point and nearest theoretical line for the given AMC. This procedure is similar to described by Walker et al. (2001).

The coefficient α and λ and β parameters were optimized using the maximum Nash-Sutcliffe modeling efficiency (*NSE*; Nash and Sutcliffe, 1970) as an objective function in the Solver tool of Microsoft Excel version 2010. Additionally, computed Q_{surf_pred} and Q_{subs_pred} runoff components of Q_{tot_pred} from the MSME model were compared to the measured pre-event initial WTE, as the AMC on the WS80 watershed with dominant Wahee soil series (Fig. 1) for identifying/detecting a WTE threshold, when the model predicted Q_{surf_pred} to test the 2nd hypothesis that there is a threshold water table elevation and precipitation amount above which overland surface runoff would occur.

The *NSE,* RMSE-observations standard deviation ratio *(RSR),* and percent bias (*PBIAS*) (Moriasi et al. 2007) were used as goodness-of-fit

Table 5
Statistical characteristics of selected rainfall-runoff events (N = 12) from the 2011–2015 period, MSME model parameters, and predicted event runoff components for Eccles Church (EC) watershed*.

Parameter	*P*	*P5*	Q_{tot_obs}	*CN*	*M*	S_a	S_b	I_{a1}	I_{a2}	Q_{surf_pred}	Q_{subs_pred}	Q_{tot_pred}
	mm	mm	mm		mm	mm	mm	mm	mm	mm	mm	Mm
Mean	61	10.9	22.1	77.5	1.47	52.1	444.9	32.4	160.1	0	15.7	15.7
Median	55.1	7.4	19.5	78	0	45.8	325.1	29.3	117.4	0	12.3	12.3
Minimum	12.2	0	1.6	60	0	18	137.5	7.6	47	0	0	0
Maximum	116.4	40.7	50.4	90	7.42	108.2	825.2	69.1	297.9	0	45.9	45.9
Standard dev.	38.2	11.9	16.6	11.9	2.74	36	291.4	23	105	0	16.1	16.1
COV	0.6	1.1	0.8	0.2	1.9	0.7	0.7	0.7	0.7	0	1	1
Kurtosis	−1.4	2.7	−1.3	−1	1.1	−0.8	−1.6	−0.8	−1.6	0	−0.7	−0.7
Skewness	0.3	1.6	0.3	−0.5	1.61	0.9	0.5	0.8	0.5	0	0.8	0.8

*All variables are explained in Table 2.

Table 6
Statistical characteristics of selected rainfall-runoff events (N = 6) from the 2011–2015 period, MSME model parameters, and predicted event runoff components for the Conifer watershed*.

Parameter	P	$P5$	Q_{tot_obs}	CN	M	S_a	S_b	I_{a1}	I_{a2}	Q_{surf_pred}	Q_{subs_pred}	Q_{tot_pred}
	mm	mm	mm		mm	mm	mm	mm	mm	mm	mm	Mm
Mean	65.9	6.6	32	83	0.76	37.7	627.3	23.6	226.2	0	25.1	25.1
Median	55.1	6.9	32.2	90	0.09	18	825.2	11.5	297.2	0	20.8	20.8
Minimum	31	0	9.9	60	0	18	137.5	9.1	49.7	0	10.3	10.3
Maximum	116.4	13	56.7	90	3.85	108.2	825.2	69.1	297.9	0	46.5	46.5
Standard dev.	35.9	5.9	17.7	12.2	1.53	36.3	312.4	23.5	112.6	0	15.2	15.2
COV	0.5	0.9	0.6	0.1	2.02	1	0.5	1	0.5	0	0.6	0.6
Kurtosis	−1.6	−2.2	−1.2	2.8	5.64	4	−1	3.9	−1	0	−1.8	−1.8
Skewness	0.7	−0.1	0.1	−1.8	2.36	2	−1.1	2	−1.1	0	0.5	0.5

*All variables are explained in Table 2.

Table 7
Statistical characteristics of selected rainfall-runoff events (N = 23) from the 2008–2011 period, MSME model parameters, and predicted event runoff components for UDC watershed*.

Parameter	P	$P5$	Q_{tot_obs}	CN	M	S_a	S_b	I_{a1}	I_{a2}	Q_{surf_pred}	Q_{subs_pred}	Q_{tot_pred}
	mm	mm	mm		mm	mm	mm	Mm	mm	Mm	mm	mm
Mean	41.7	13.5	3.7	69.1	2.1	78.1	249.6	48.5	90.1	0	1.2	1.2
Median	35	6	2	75	0	54.1	275.1	34.6	99.3	0	0	0
Minimum	22	0	0	57	0	22.1	121.5	10.3	43.9	0	0	0
Maximum	87	81	12	88	21	122.4	672.4	78.2	242.7	0	9.8	9.8
Standard dev.	21.1	19.5	4.1	10.6	4.9	37.5	152.7	24.8	55.1	0	2.8	2.8
COV	0.5	1.4	1.1	0.2	2.3	0.5	0.6	0.5	0.6	0	2.3	2.3
Kurtosis	−0.4	5.7	−0.4	−1.2	10.4	−1.7	3.8	−1.7	3.8	0	6.7	6.7
Skewness	1	2.2	0.9	0	3.1	0.3	1.9	0.2	1.9	0	2.7	2.7

*All variables are explained in Table 2.

measures to assess the performance of the models in predicting direct outflow using the Ritter and Muñoz-Carpena (2013) criteria for the *NSE*, with satisfactory performance for $NSE > 0.65$, good performance for $NSE > 0.80$, and very good performance for $NSE > 0.90$.

We also conducted an uncertainty analysis of simulated event Q_{tot_pred} predicted by the MSME model on the WS80 watershed based on the generalized likelihood uncertainty estimation (GLUE) method. The procedure is based on running Monte Carlo (MC) model simulations with different parameter sets. The parameter sets were sampled from proposed (prior) distributions, and the simulated outputs and parameter (posterior) distributions were inferred to identify the closest fit to the observations obtained from parameter sets defined as "behavioral" (Blasone et al., 2008). *A priori* "uniform" distribution of the α model coefficient was assumed based on the observed events for generating random values for the MC simulation run. Again, the *NSE* statistic was chosen for the likelihood function. To provide a quantitative evaluation of the difference among the results, the following uncertainties were calculated:

- Average Relative Interval Length (ARIL) proposed by Jin et al. (2010):

$$ARIL = \frac{1}{n}\sum_{i=1}^{n}\frac{Limit_{u,t} - Limit_{l,t}}{Q_{tot\_obs,t}} \tag{1}$$

- Average Asymmetry Degree (AAD) of the prediction bounds with respect to the corresponding observed discharge proposed by (Xiong et al. 2009),

$$AAD = \frac{1}{n}\sum_{i=1}^{n}\left|\frac{Limit_{u,t} - Q_{tot\_obs,t}}{Limit_{u,t} - Limit_{l,t}} - 0.5\right| \tag{2}$$

- And Average Deviation Amplitude (ADA) proposed by Xiong et al. (2009):

$$ADA = \frac{1}{n}\sum_{i=1}^{n}\left|\frac{1}{2}\left(Limit_{u,t} + Limit_{l,t}\right) - Q_{tot\_obs,t}\right| \tag{3}$$

where: $Limit_{l,t}$ and $Limit_{u,t}$ are the lower and upper boundary values of 95% confidence intervals, $Q_{tot\_obs,t}$ is the total observed runoff, and n is the number of time steps.

Additionally, the percentages of observations that are contained in the calculated 95% confidence intervals (Jin et al., 2010) were also calculated as:

$$P - 95CI = \frac{NQ_i}{n} \bullet 100\% \tag{4}$$

where n is the number of events and NQ_i is the number of observations that are contained in the calculated confidence intervals.

Finally, we applied the MSME model, without any calibration, to predict the Q_{tot_pred} on Eccles Church and Conifer watersheds with 12 and 6 storm events, respectively, and in sandy UDC watershed with 23 events for the model validation. We also assumed the same value of α coefficient calibrated for the WS80 watershed for predicting Q_{tot_pred} on all the three watersheds, as a part of the same hypothesis, to demonstrate that the MSME model can generate the Q_{tot_pred} and its surface and subsurface components from varying coastal forest watersheds.

3. Results and discussion

3.1. Storm event hydrograph characteristics

Data in Table 2 shows the values and statistics of measured rainfall-runoff storm event parameters used in the MSME model for the 2008–2015 period for the WS80 watershed. The average and maximum event precipitation (P) for the period amounted to 73.1 mm and 157.7 mm, respectively. The observed direct runoff (Q_{tot_obs}) response to rainfall events varied from zero to 88 mm, with an average of 13.2 mm (Table 2). The 5-day prior rainfall ($P5$) showed some variability (COV) (Table 2). The large values of kurtosis and skewness and the difference

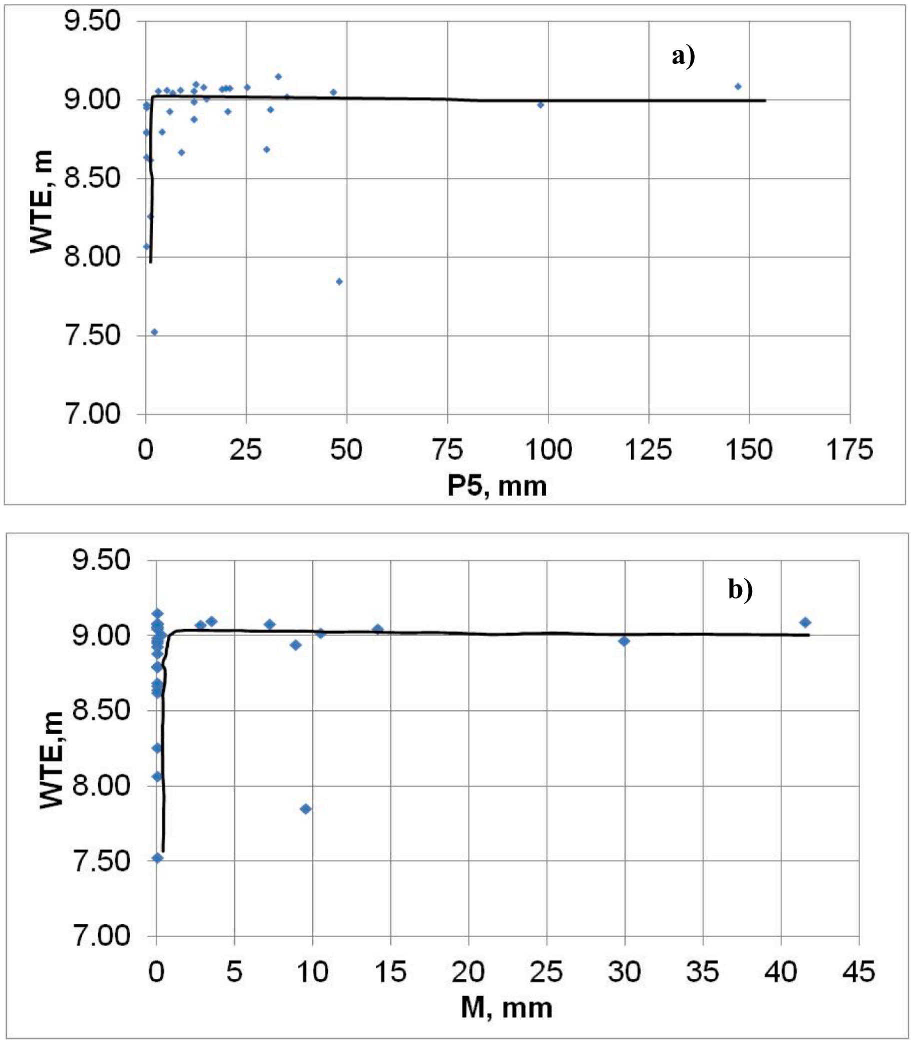

Fig. 3. Relationships between a) water table elevation (WTE) and *P5* and b) WTE and antecedent soil moisture (M) on WS80 watershed; the solid black line represents the average fitted relationship.

between the mean and the median show an asymmetric distribution of most of the *P* and Q_{tot_obs} parameters to the right (Table 2). The value of kurtosis suggests most of *P* and Q_{tot_obs} values were grouped about the mean value while the skewness shows that more events have rainfall and runoff less than their respective mean value.

3.2. MSME Modeling of Surface and Subsurface Runoff in WS80 watershed

The MSME model-predicted mean total runoff ($Q_{tot\,pred}$) value across 36 storms for the 2008–2015 period was 11.0 mm, close to the observed value of 13.2 mm, with no significant difference (t test = -0.787, $p = 0.436 > \alpha = 0.05$) (Table 2). The analysis was based on the weighted *CN* taken from the published NRCS table (USDA, 1986) but modified with the AMC, with a mean of 66.7 (57.0–88.0), which was almost the same as the value of 68, reported earlier by Epps et al. (2013b), after adjustment of the antecedent soil moisture (ASM) defined by WT for selected storm events on the WS80 watershed (Table 1).

Mean ASM, expressed by the *M* parameter (eq. A(4)), was equal to $M = 3.6$ mm with a range of 0.0–41.5 and represents soil moisture index for very thin soil layer added by *P5* rainfall (Table 2). The lower initial soil moisture on the WS80 watershed was supported by the lower mean initial WTE (Fig. 3). It is evident from the asymptotic nature of the plots in Fig. 3a and 3b that the WTE attains its highest value at nearly 9 m and remains stable, but at a single well location on the watershed, for M > 1.0 mm. This result tends to indicate that there may possibly be a watershed-wide threshold value of the shallow WTE within an uncertainty range due to varying microtopography (Amoah et al., 2013), when soils attain high antecedent moisture with saturation (hypothesis 2). This relationship is also consistent with Amatya et al. (2020) who reported all high water table soils generally respond similarly to extreme precipitation events.

As a next step, we examined the influence of *P5* antecedent rainfall on WTE in Fig. 3a. Apparently, for a small increase in values of *P5*, WTE increases rapidly attaining a maximum WTE after *P5* reaches a threshold of 3.0 mm. The WTE has lesser variability for any M values higher than the threshold value (Fig. 3b). Therefore, more water added to an already saturated soil cannot infiltrate further into the soil, and causes ponding and generating higher overland surface runoff than the subsurface.

Computed results showed that the average Q_{subs_pred} was larger than the average $Q_{surf\,pred}$ on the WS80 watershed (Table 2), consistent with Amatya et al. (1996) study who reported that it is rare in low-gradient watersheds for Q_{surf} to occur, but may occur, for example, after large two-year recurrence storm events exceeding 100 mm of rainfall in 24 hrs (Amatya et al., 1998).

Relationships between rainfall and computed runoff for all events on the WS80 watershed are presented in Fig. 4. Initial WTEs were also plotted for the corresponding events for WS80 in Fig. 4a, which shows,

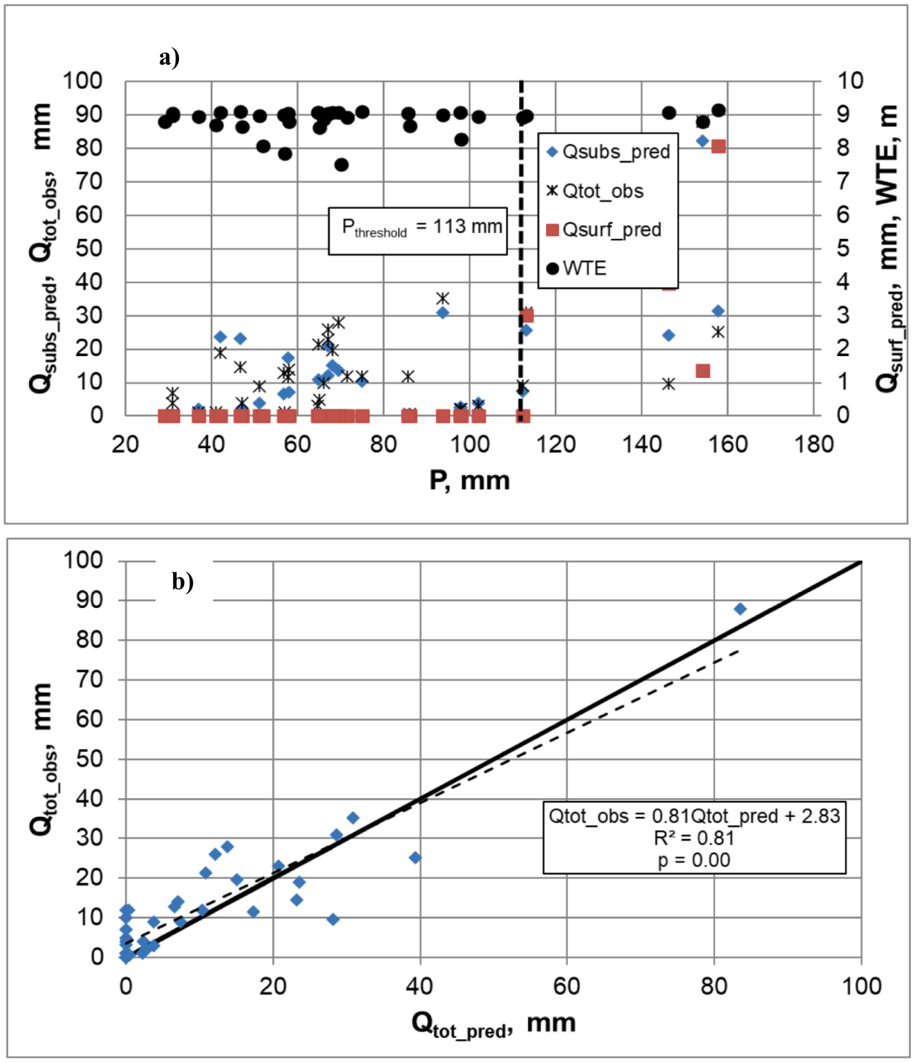

Fig. 4. Relationships for the WS80 watershed between a) measured event total rainfall (P) and observed direct runoff (Q_{tot_obs}), predicted saturated subsurface runoff (Q_{subs_pred}), predicted overland surface runoff (Q_{surf_pred}) and water table elevation (WTE) and b) Q_{tot_obs} and predicted runoff (Q_{tot_pred}) for rainfall-runoff events, with a solid black line for 1:1 relationship. The dashed line in Fig. 4b represents the regression line with R^2 (coefficient of determination) and a p value.

despite the WTE achieved threshold of 9.00 m or somewhat higher, only Q_{subs_pred} was observed (left side of the vertical line in Fig. 4a). On the other hand, the Q_{surf_pred} runoff was generated by the MSME model only when P threshold of 113 mm was achieved. Accordingly, we can conclude that it is the rainfall together with AMC, not WTE alone, is a crucial factor determining generation of overland flow in this flat coastal watershed. Accordingly, when the high WTE near 9.0 m was linked with corresponding high event rainfall, the model generated highest Q_{tot_pred}. When the P was below detected threshold, only Q_{subs_pred} was predicted on the watershed. The P threshold on the WS80 watershed was equal to 113 mm, supporting our 2nd hypothesis. However, there was no data on individual Q components to verify although this qualitatively supports the Harder et al (2007) study who reported that when the WT positions at their single study well were at<0.1 m depth at the onset of the storm event, the saturated conditions should cause a large fraction of the rainfall to leave the system as surface and shallow subsurface runoff. A similar concept of pre-threshold runoff as subsurface and threshold excess runoff in the SCS-CN method was proposed by Bartlett et al. (2016) for simulating runoff generation in hillslope hydrology dominated forest watersheds. However, additional field studies are needed to verify the generation of separate Q_{sub} and Q_{surf} components for the runoff events as only the total direct runoff (Q) was measured at the site.

Parameters of the calibrated MSME model and computed measures of goodness-of-fit for model performance compared to the observed data are given in Table 3 for WS80 watershed and additionally for three other validated watersheds: Eccles Church, Conifer, and the UDC. The coefficient, α, obtained from the calibration, was found to be equal to 0.639 for the WS80 watershed. The value of $\beta = 0.703$ indicated that the ASM index (M) at the beginning of the rain event was not only likely caused by infiltrating rainfall as defined by $P5$ but also by the WTE, as a surrogate of soil moisture, because a portion of $P5$ would have been lost by ET (Amatya et al. 2020). The model performance statistics of RSR and NSE calculated as 0.44 and 0.80, respectively, were classified as “good” for NSE according to Ritter and Muñoz-Carpena (2013) criteria. These results are also better than those from the previous versions of the model (SME_m and others) on the WS80 watershed. For example, Walega et al. (2020) obtained an NSE of 0.72 using the SME_m model and 0.73 for the original SCS-CN model using the CN based on USDA (2004) on this watershed. However, Walega et al. (2017) had reported slightly better performance of the Mishra-Sahu (MS) model compared to the Sahu 1 and 3 parameter models on this watershed. The positive value of PBIAS suggests the average tendency of the simulated data to slightly underestimate total direct runoff to their observed counterparts.

Comparing the predicted event total runoff (Q_{tot_pred}) to the observed data (Fig. 4b) shows a good agreement for the WS80 watershed, supporting the 1st hypothesis. However, predicted Q_{tot_pred} values are

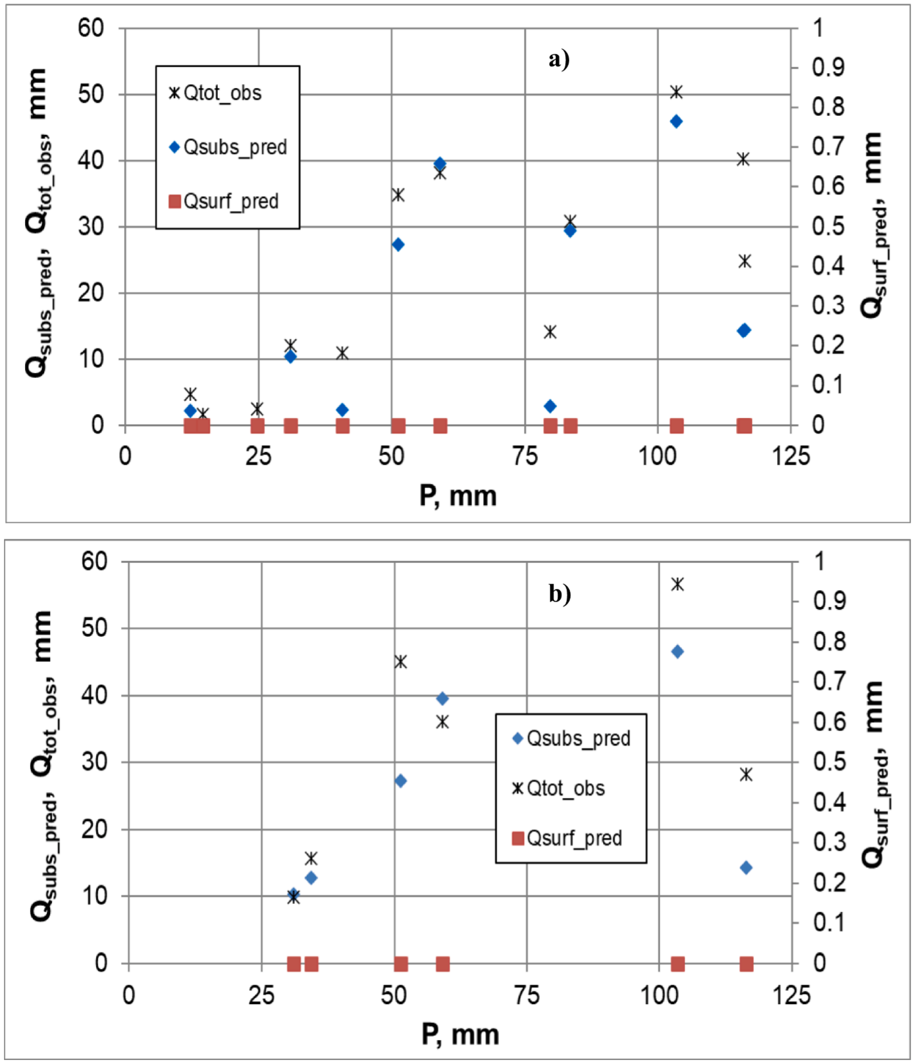

Fig. 5. Relationships between measured event total rainfall (P) and observed direct runoff (Q_{tot_obs}), predicted saturated subsurface runoff (Q_{subs_pred}), and predicted overland surface runoff (Q_{surf_pred}) for a) Eccles Church and b) Conifer watersheds.

slightly lower than those observed in the case of larger runoff events. This may be likely due to slightly lower weighted CN value (66.7), obtained from the USDA (2004) to include in the MSME model (Table 2), compared to the CN of 68 obtained after adjusting for the AMC defined by the WT at the site as reported in Epps et al. (2013b) study.

3.3. Uncertainty of the MSME model

The uncertainty of the MSME model predictions was analyzed for the storm events on the WS80 watershed to detect the potential influence of the α coefficient on prediction errors of simulations. A selection criterion for the α coefficient was the threshold value of the likelihood function with the *NSE* value exceeding 0.65, which, as previously mentioned, was deemed satisfactory. The simulations in which the *NSE* values were below 0.65 were excluded from further analysis. To provide a broad quantitative evaluation of the uncertainty analysis, simulations results from *ARIL*, *AAD*, and *ADA* statistical criteria were calculated (Table 4). The calculated value of $ARIL = 0.496$ is in a somewhat similar range reported in other literature (0.09 to 1.30) for monthly nitrate load and storm hydrograph predictions (Appling et al., 2015; Walega and Książek, 2016), indicating relatively lower uncertainties in the model predictions. An *AAD* value lower than 0.50 indicates that, on average, the observed runoff was within the prediction uncertainty bands, whereas the higher the *AAD* value, the more asymmetrical the uncertainty bands were around the observed water levels (Xiong et al. 2009; Walega and Książek 2016). Our calculations showed the *AAD* value of 0.797 (Table 4) was slightly higher than 0.50 but substantially lower than 1.32 obtained by Walega and Książek (2016), suggesting that the average observed runoff is likely higher than the upper uncertainty band.

P-95 CI statistics used to quantify the random and systematic errors in simulations indicate that the *P-95 CI* values > 50 % stand for more random errors, whereas the *P-95 CI* values < 50 % suggest systematic errors, as sources of uncertainties in simulations. As shown in Table 3, our calculated *P-95 CI* value of 44.44% is slightly lower than 50%, indicating a slight potential for systematic errors in the MSME modeling results. The plot in Fig. 2b shows the model's tendency to slightly underpredict the events, particularly those with deeper WTEs. However, this systematic average error of 15% overprediction of runoff, with a range of 8.7 to 20.2% was deemed acceptable considering other potential errors in the estimated *CN* parameter as well as in the measured data. Also, this was likely due to predicted narrow bands of uncertainty caused by narrow variability of the accepted α coefficient assuming a uniform Wahee soil throughout the watershed, which has some heterogeneities (Fig. 1). This means the model may have insufficiently captured changes of ASM across the watershed. However, this potential WTE threshold from localized well data on the Wahee soil may not be quite representative of the whole watershed with some additional soil types, consistent with Bartlett et al. (2016) for addressing

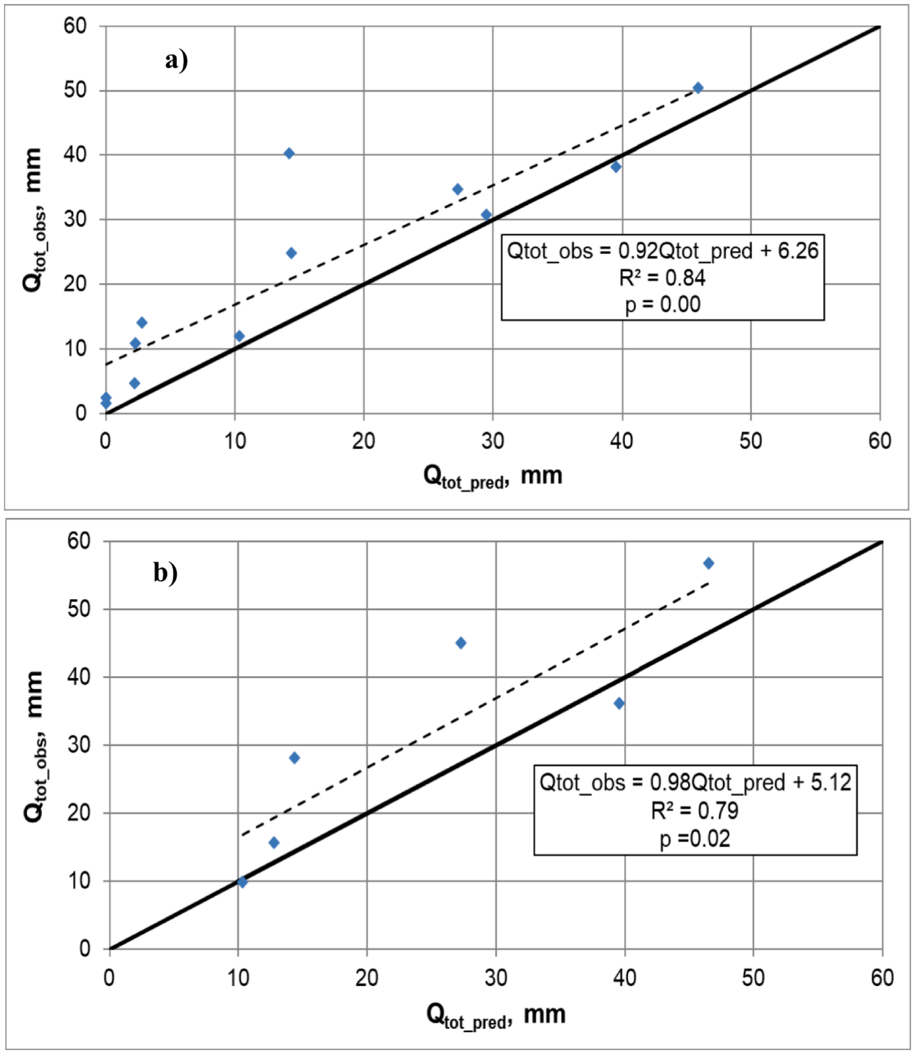

Fig. 6. Relationship between Q_{tot_obs} and Q_{tot_pred} for rainfall-runoff events on a) Eccles Church and b) Conifer watersheds. The solid black lines represent a 1:1 relationship and the dashed lines represent regression lines with R^2 (coefficient of determination) and *p* value.

heterogeneities for large areas.

3.4. Validation of MSME model on two other watersheds with relatively poorly drained low permeability soils

Observed data and computed statistics of rainfall-runoff parameters for the MSME model for the Eccles Church and Conifer watersheds for the 2011–2015 period are shown in Tables 5 and 6, respectively. The average event *P* of 61.0 mm for Eccles Church is slightly lower than the 65.9 mm for the Conifer watershed and much lower than for WS80 (Table 2), but similar maximum values were observed for the Eccles Church and Conifer sites. The 5-day prior *P5* is lesser on Eccles Church and Conifer watersheds compared to the WS80 watershed. The observed average outflows (Q_{tot_obs}) were 22.1 mm, 32.0 mm, and 13.2 mm for the Eccles Church, Conifer, and WS80 watersheds, respectively.

Mean *CN* values, obtained from the USDA (1986) and modified for the AMCs, for the Eccles Church and Conifer watersheds were found to be 77.5 and 83, respectively, with a range of 60–90 for both (Tables 5 and 6). *CN* was higher on the Conifer watershed than the Eccles Church watershed, as expected, due to relatively well-drained soils on Eccles Church with a potential for a larger initial abstraction relative to the Conifer watershed. The *M* index for the validated watersheds Eccles Church on sandy soils and the Conifer on loamy clay soils were smaller than on WS80 watershed (Tables 2, 5, 6), with a large field capacity and low permeability soils in addition to the largest wetland area (Harder et al., 2007 - Table 1).

Relationships between rainfall and computed runoff for all events on Eccles Church and Conifer watersheds are presented in Fig. 5.

The influence of rainfall (*P*) on the runoff (Q_{tot_obs}) is evident. The analysis showed a lack of overland surface runoff on both the Eccles and Conifer watersheds including for larger rainfall events. We assumed the WTE threshold at saturation for the Eccles Church on Lynchburg soils and Conifer on Wahee soil similar to that on WS80, because both the Wahee and Lynchburg soils are classified as somewhat poorly drained located in the same low-gradient topographical and geological conditions. Also, both soils are similar texture-wise as fine sandy loam and fine loamy sand and have three out of five similar terms in taxonomy (semi-active, thermic, Aeric) (Williams and Amatya, 2016). In addition, when the soils are saturated with WTE near or at the surface, both soils respond similarly during high rainfall events (Amatya et al., 2020).

Comparisons of the predicted event total runoff (Q_{tot_pred}) to the observed data for the Eccles Church and Conifer watersheds plotted in Fig. 6a and 6b, respectively, show a relatively poorer agreement for both the watersheds compared to WS80 (Fig. 4b), with slightly lower predicted *Q* values than the observed although the computed statistics showed a satisfactory performance (Table 3). Positive values of *PBIAS* in both watersheds suggest that the MSME model tends to underestimate mean direct runoff as much as 29% compared to the observed. The fact,

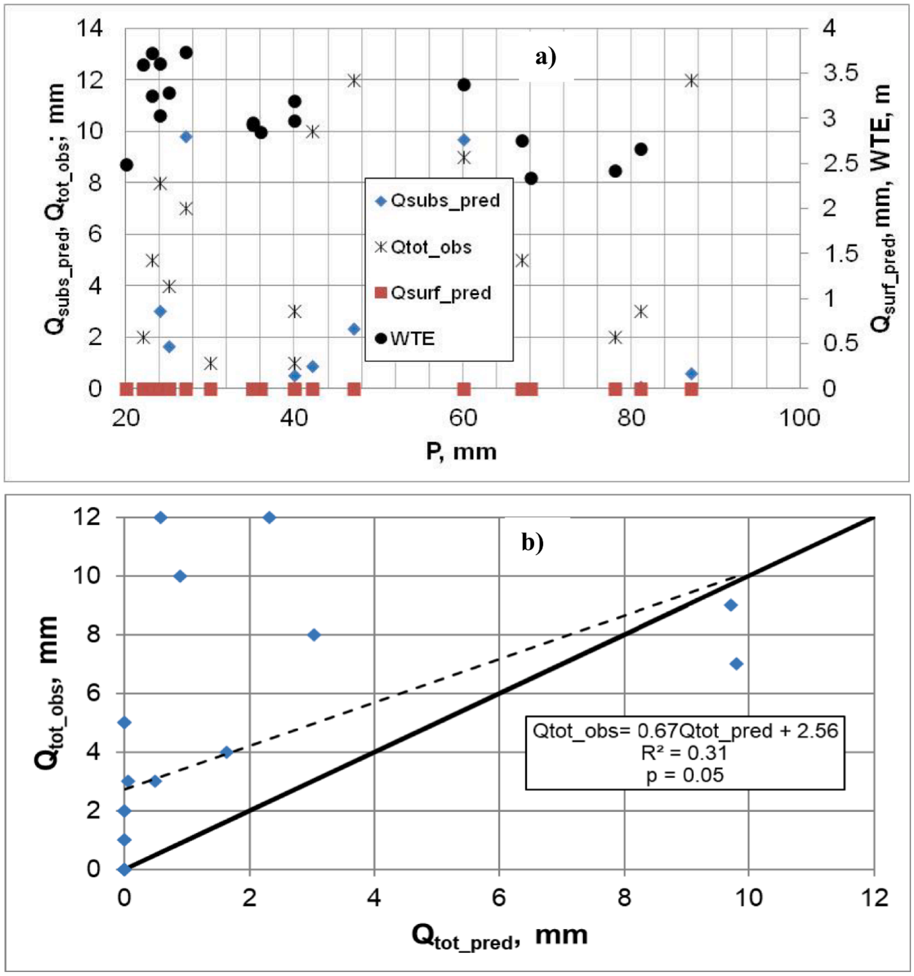

Fig. 7. Relationships for the UDC watershed between: a) measured total event rainfall (*P*) and predicted total surface runoff ($Q_{tot\ pred}$) and its components and b) relationship between $Q_{tot\ obs}$ and $Q_{tot\ pred}$ for rainfall-runoff events, with a solid black line for 1:1 relationship. The dashed line in Fig. 7b represents the regression line with R^2 (coefficient of determination) and a *p* value.

that the model performance of simulating $Q_{tot\ pred}$ was satisfactory based on evaluation statistics (Table 3; Fig. 6), suggests that the MSME model, using the published NCRS CN values and calibrated with parameters from a watershed with long-term data, can be used for simulating event rainfall-runoff in ungauged watersheds with similar conditions.

3.5. Validation of the MSME model on a watershed with high permeability soils

The predicted values and statistics of rainfall-runoff parameters for the MSME model for the 2008–2011 period for the UDC watershed are shown in Table 7 together with observed rainfall and runoff data. The average event *P* of 41.7 mm was much less than that for previously described watersheds despite the slightly higher 5-day prior rainfall than for the Eccles Church and Conifer watersheds but less compared to the WS80 watershed. The smallest observed average $Q_{tot\ obs}$ of 3.7 mm on UDC, the smallest value for all the four watersheds, was likely due to the larger permeability of the sandy soils of Lynn Haven and Leon series (Epps et al., 2013a).

The calculated *CN* mean for the UDC watersheds was 69.1, with a range of 57.0–88.0, which was substantially lower than the *CN* values for the Conifer and Eccles Church watersheds (Tables 5 and 6) but slightly higher than the values reported by Epps et al. (2013b). However, the ASM index (*M)* values for this validated watershed were similar to that of the WS80 watershed (Tables 2 and 7).

The relationship between *P* and computed $Q_{tot\ pred}$ and its components for all storm events on the UDC watershed are presented in Fig. 7a.

The plot and the analysis showed that the MSME model, using the α coefficient as on the WS80, did not yield surface overland runoff in any of the storm events but only the shallow subsurface saturated runoff on this watershed with highly permeable soil. This result is consistent with Slattery et al. (2006), who showed that the subsurface flow is dominant where there are deep, permeable soils. The plot in Fig. 7a also shows an increase in $Q_{subs\ pred}$ values with an increase in WTEs, consistent with other studies (Harder et al., 2007). As a result, total runoff from the UDC watershed was simulated as shallow subsurface saturated runoff only. The MSME model for this watershed performed poorer (NSE = -0.13) than for the other watersheds (Table 2), with an unsatisfactory performance using the Ritter and Carpena (2013) criterion. The poor quality of the model is also evident from the calculated *RSR* and *PBIAS* measures. High *PBIAS* suggests that total direct runoff predicted by the MSME model is substantially underestimated compared to observed events. The poor results of runoff achieved from the MSME model in the UDC watershed can be attributed to the underestimation of the antecedent soil moisture *M* for high permeability soil. The initial abstractions I_{a1} and I_{a2} were too large, and thus losses of rainfall *P* caused the predicted runoff from the MSME model to be significantly smaller than the observed. Thus, we conclude that the MSME model, without any calibration, is not able to reasonably predict total direct runoff formation from storm events on this watershed with higher soil permeability (Fig. 7b).

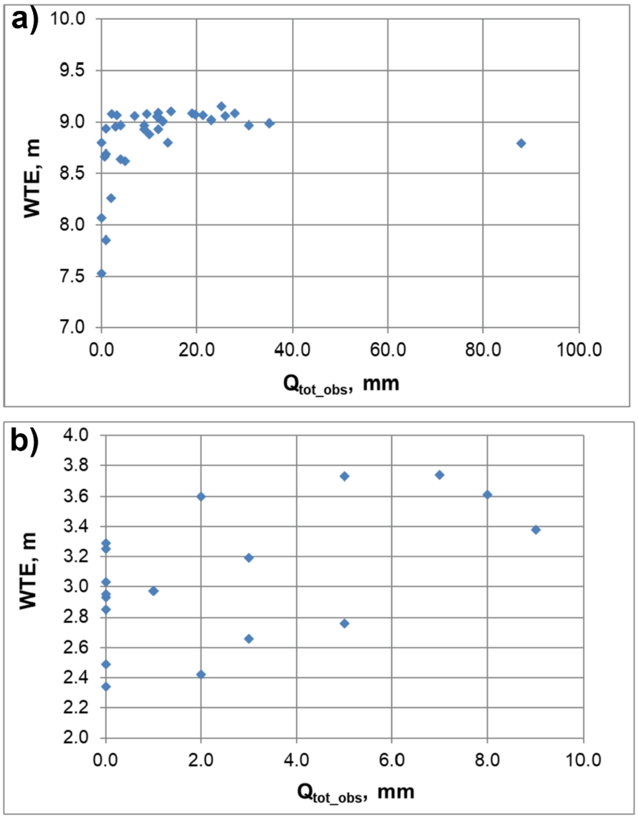

Fig. 8. Relationship between WTE and observed total runoff for a) WS80 and b) UDC watersheds.

3.6. Interpretations of runoff response for storm event modeling and future works

3.6.1. Water Table threshold on partitioning subsurface saturated and surface overland runoff

In this study, we found the model predicted shallow subsurface saturated flow as "streamside" runoff for all storm events on all four watersheds. Only on WS80, when a threshold of 113 mm precipitation was exceeded, the model predicted surface overland "watershedwide" runoff. The results on the WS80 are consistent with other forested catchments (Juez et al., 2021; Wilcox et al., 2011). For example, Juez et al. (2021) studied hydrological dynamics in forested catchments in San Salvador Central Spanish Pyrenees and detected a rainfall threshold of 105.8 mm, above which high-magnitude low-frequency events were observed with the rainfall-runoff slope considerably stronger than the observed under the threshold. The same authors also concluded that the

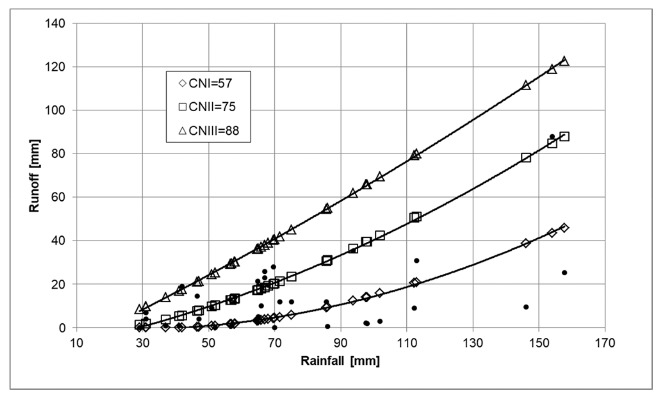

Fig. B1. The observed rainfall-runoff events and direct outflow calculated according to SCS-CN method for different CN values, corresponding to three antecedent moisture conditions for WS80 watershed.

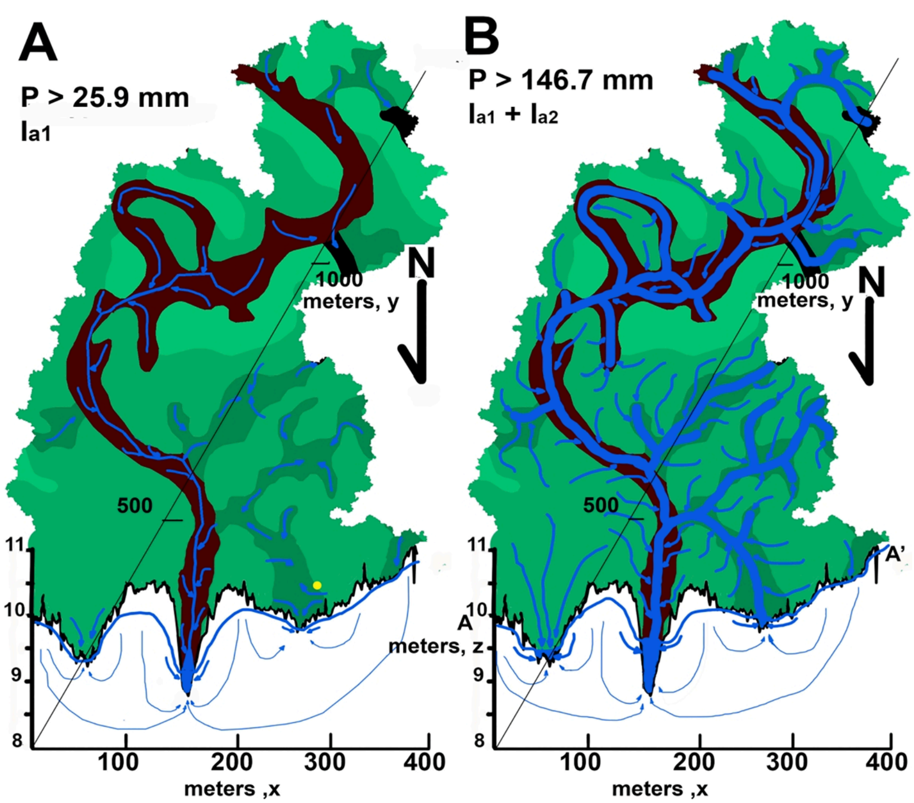

Fig. 9. Conceptual diagram of runoff generation on a pseudo-3D representation of the Eccles Church watershed. MSME model estimates of initial abstraction (average values of I_{a1} and I_{a2} in Table 5) are related to: A) situation where only subsurface runoff occurs near the channel and B) where streamside runoff extends, by an expanding channel system, across most of the watershed to become watershed-wide overland surface runoff. Arrow sizes reflect the volume of runoff. This figure is derived from Fig. 1c as a cross-section relating to transect line A-A' and a plan view upstream to the south.

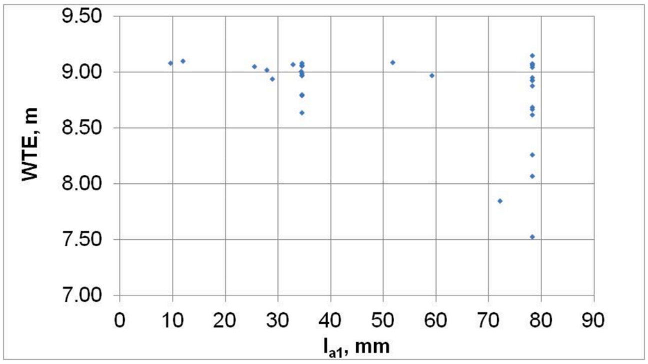

Fig. B2. Relationships between WTE and I_{a1} in WS80 watershed

catchment response is related to the height of the water table, which in turn was related to antecedent rainfall conditions, similar to our results. The MSME model assumes that watershedwide surface overland runoff is initiated when the watershed is completely saturated in a situation when *P5* corresponds to the maximum potential retention.

This study did not find a threshold relationship for WTE above which surface overland runoff would likely be generated by the MSME model. The model yielded only subsurface saturated runoff even for the WTE of 9.0 m or above (Fig. 4a) at a single well location on WS80. On the other hand a WTE of approximately 9.0 m in a well on WS80 suggests that there may possibly be a threshold WTE value when soils attain high antecedent moisture with saturation across the watershed (Fig. 3) thus producing increased total runoff. This hypothesis for WS80 is supported by WTE versus observed total runoff Q plot in Fig. 8a but did not hold true for the well on the UDC watershed (Fig. 8b). Detection of a relationship between WTE and runoff could dictate the rainfall response on these watersheds between dry and wet ASM. As mentioned early, WTE can influence on soil moisture and thus on possible runoff generation.

As shown in Fig. B2, WTE elevation is linked with Ia1, representing initial abstraction for subsurface saturated runoff. Initially when WTE is close to the surface, Ia1 has lower value but after rain events the value exceeds Ia1, resulting in formation of subsurface runoff. For deeper WTE, Ia1 is also decreased, potentially with also the decreased chance of the subsurface runoff occurrence. Moreover, according to equation A(2), the Ia1 is determined by antecedent soil moisture M. For example, if M increases yielding higher moisture, Ia1 decreases, and thus also the storage decreases. This behavior consequently pronounces the subsurface runoff generation process. In this case both the WTE and Ia2 do not yield similar behavior, confirming that occurrence of surface overland runoff is more determined by rainfall depth than the WTE. For example, in their study on this watershed, Epps et al. (2013a) showed that only very moderate amounts of runoff could be expected for rain events that occur when the WTE is below a threshold as dry ASM. On the other hand, substantial watershed-wide runoff generation might be expected under high WTE across the watershed, exceeding a representative of threshold, consistent with Harder et al. (2007), who found exponentially increasing runoff when the water table was ponded>40 mm at a given well location on the WS80 watershed.

All three studies found a threshold rainfall to runoff response when the WTE at the WS80 observation well reached near 9 m, which was close to the soil surface at that location. However, we expect some variation in this single well-based threshold on a watershed-scale basis for this watershed with a mean depressional storage of 93 mm (87 – 99 mm) (Amoah et al., 2013).

The UDC watershed demonstrates how WTE is a site specific varible. UDC has an elevation range of 1.8 – 6.5 m (Table 2) indicating a WTE of 9 m is impossible at this site. The relationship for the observations at UDC (Fig. 8b) indicates 7 out of 17 events, with WTE ranging from 2.3 to 3.3 m, result in no runoff and higher rates of runoff are associated with WTE over 3.4 m. The sandy subsoils of UDC have much less moisture holding capacity and unsaturated storage is quite small. In this case, threshold behavior occurs over a broader range of WTE from 3.4 to 3.8 m (Epps et al 2013a) and half of the observed storm with runoff were above the 3.4 m value of WTE.

3.6.2. Soil saturation coefficient α

The coefficient α in the MSME model can be interpreted as the partial area contribution of saturated soil. That coefficient plays an important role in predicting the switching from Q_{subs_pred} to Q_{surf_pred} runoff. In this way, the MSME model may be mimicking saturation excess overland flow (Dunne and Black, 1970). The relationship of α to both a threshold rainfall amount and a specific WTE on WS80 suggests the calibrated coefficients of the lumped MSME may relate to a spatially distributed saturation excess overland flow generation process (Dunne et al., 1975). The role of soil saturation (water table depth or elevation) in runoff threshold behavior has been recognized in coastal forested watersheds for decades (Epps et al., 2013a; Eshleman et al., 1994; Harder et al., 2007; Williams, 1979; Williams, 2007). Yet those studies, like this one, used a single well elevation as an index to infer the spatially distributed water table.

Siebert et al. (2011) determined that a major source of runoff generation, in Swedish peat-dominated low gradient forested watersheds, was the high conductivity of the surface forest floor and upper peat layers. McDonnell et al (1991) also found high horizontal conductivity in the forest floor on steep forested watersheds in New Zealand. They discounted the mechanism as a source of runoff in those watersheds, as rapid flow could only be measured over a distance of a few tens of meters. Bishop et al. (1990) found that the flow in the Swedish streams could be accounted for by this shallow flow in a region within 30 m of the stream. Skaggs et al. (2016) found similar apparent high surface hydraulic conductivity in North Carolina, but a tenfold decrease after bedding destroyed the forest floor. Walega and Amatya (2020) used data from an undisturbed, but artificially-drained, forested watershed in coastal North Carolina in the development of the MSME model. That model indicated that the shallow subsurface mechanism occurred within 50 m of the stream. Can the results of the MSME model be used to create a hypothesis of how a shallow subsurface flow mechanism may be active on undrained coastal forested watersheds?

The Eccles Church watershed can be used to visualize the above hypothesis (Fig. 9). Eccles Church is located on a Pleistocene aged floodplain (Colquhoun 1974) where soils have developed on the former floodplain surface. The stream has developed in an old meander scar while other poorly drained soils are found in micro-topographic lows based on an overlay of soils with a LiDAR-based digital elevation model (DEM) of the area (Amatya et al., 2015). Using the MSME model results for this watershed (Table 5), we can visualize a condition similar to Fig. 9a after 25.9 mm of rain during median conditions. With that rainfall, rapid subsurface flow occurs only on the most poorly drained portions of the watershed and drains to the closest topographic low, and limited area near the stream contributes to stream flow. The model also suggests that the condition of Fig. 9a may occur after only 7.6 mm of rainfall during wet conditions or as much as 69.1 mm during dry conditions.

Similarly, the model predicts conditions of Fig. 9b will occur after 146.7 mm of rain in median conditions. In this case, the rapid shallow subsurface flow will be extensive on all but the well-drained soils and the topographic lows will connect to the stream forming a continuous saturated zone across much of the watershed. As shown earlier in Fig. 2, one could visualize the model component I_{a1} to represent the rainfall needed to trigger rapid subsurface flow, and I_{a2} to be the additional rainfall needed before all the topographic lows are connected to the outlet. The model results suggest the initiation of this watershedwide runoff may occur after as little as 55 mm during wet conditions or only after 366 mm during very dry periods.

These findings suggest the need for attention to varying parameters and initial conditions when modeling storm runoff in wetland-rich low-gradient watersheds in the southeastern U.S. For example, initial WTE and soil moisture, if available, should be investigated on soil texture and drainage class basis as the parameters calibrated on the WS80 were validated satisfactorily on two other watersheds with clay and clay loam subsoil, but performed rather poorly for a watershed with sandy subsoil and very low relief in the same region. Accounting for these initial conditions is one of the key advantages of applying the CN-based models, including the MSME model also with watershedwide overland surface and streamside shallow subsurface saturated runoff partitioning methods used in this study, over the widely used original SCS-CN method. However, the uncertainty analysis of simulated direct runoff due to the α coefficient in the MSME model showed systematic errors with some overpredictions of observed runoff events. The values of α were less variable due to the small variability in WTE above the 9.00 m (soil saturation), resulting in overland surface runoff based on a single well data on the dominant soil of the WS80 watershed. These results demonstrate the need for model validation with multiple soil types and topography even in the low-gradient system to reduce prediction uncertainties for the general application of the model in similar other regions.

We recognize this is a more intensive field approach, yet it yielded more detailed independent data for components of stormflow itself, besides the purpose of stormflow/baseflow separation of streamflow. This is important for calibrating runoff models applied in the design of stormwater management practices in these coastal landscapes facing urbanization and climate change effects including extreme rainfall events (Amatya et al., 2021; Corbin et al., 2022). Future research may also consider the MSME model integrated with empirical rainfall-runoff models like Soil Conservation Service – Unit Hydrograph (SCS-UH) and/or EBA4SUB model (Petroselli, 2020) to include surface and subsurface runoff in design hydrograph generation and test the approach in multiple watersheds with varying slopes and land cover. Another recommended aspect of future studies is to focus on the α parameter and its linkage with a parameter describing groundwater and/or soil moisture, as was described by Camporese et al. (2019) who used Topographic Wetness Indices (TWI) to determine the value of the α parameter. Similar linkage including those derived using recent ultra-high resolution remote sensing-based soil moisture images (Ma et al., 2020) is also a possibility with the MSME model to reliably predict direct surface runoff in an ungauged forest and rural watersheds.

4. Summary and conclusions

Storm event direct runoff Q_{tot_pred} was evaluated on three small, forested watersheds (115, 160, and 210 ha) at the USDA Forest Service Francis Marion National Forest and a fourth watershed (100 ha) near Georgetown and North Inlet-Winyah Bay, all in the rapidly urbanizing lower coastal plain of South Carolina, USA. The watersheds had different dominant soil types with varying drainage classes, but similar forest management practices. We analyzed and satisfactorily calibrated the interrelationships of the Q_{tot_obs} and event rainfall predicted using the modified Mishra-Sahu-Eldo (MSME) model mechanisms for the 160-ha watershed. This was performed in conjunction with published NRCS CN values and other event parameters including antecedent moisture conditions defined by rainfall and water table elevation using data collected from multiple storm events that occurred between 2008 and 2015. Also, we found that water table elevation can be linked with α parameter, in the MSME model, which can be interpreted as a soil saturation coefficient obtained by calibration for approximating the proportion of watershed area with saturated soil profile to partition watershedwide overland surface (Q_{surf_pred}) and subsurface saturated (Q_{subs_pred}) runoff. The uncertainty analysis showed that systematic error due to this parameter can be a significant source of Q prediction uncertainty. Model validation using the same α parameter and event data for the 2008–2011 period on the 100-ha watershed and the 2011–2015 period on two other watersheds (110 ha and 210 ha) showed satisfactory performance of the MSME model in predicting direct runoff only on the two poorly drained watersheds but not on the 100-ha watershed with higher soil permeability. Our results showed that Q_{surf_pred} is triggered only after rainfall reaches threshold values of 113 mm, on WS80 but not on Eccles and Conifer watersheds with limited event data compared to WS80. Results of this study suggest that the MSME model can be used for adequately estimating total direct runoff on poorly drained coastal sites with similar characteristics as the study sites. In addition, the model has the potential to be used in partitioning the direct runoff and estimating peak discharge estimates for the design of road drainage and stormwater management practices in the face of changing land use and climate in coastal watersheds with low-gradient topography and shallow water table soils.

CRediT authorship contribution statement

D.M. Amatya: Conceptualization, Methodology, Formal analysis, Investigation, Data curation, Writing – original draft, Writing – review & editing, Visualization, Supervision, Project administration. **A. Walega:** Conceptualization, Methodology, Software, Formal analysis, Writing – original draft, Writing – review & editing, Visualization. **T.J. Callahan:** Conceptualization, Methodology, Formal analysis, Investigation, Data curation, Writing – original draft, Writing – review & editing, Visualization. **A. Morrison:** Software, Formal analysis, Investigation, Data curation. **V. Vulava:** Writing – original draft, Writing – review & editing. **D.R. Hitchcock:** Methodology, Investigation, Data curation, Writing – original draft, Writing – review & editing. **T.M. Williams:** Conceptualization, Methodology, Software, Formal analysis, Data curation, Writing – original draft, Visualization. **T. Epps:** Methodology, Software, Formal analysis, Investigation, Writing – original draft.

Declaration of Competing Interest

The authors declare that they have no known competing financial interests or personal relationships that could have appeared to influence the work reported in this paper.

Acknowledgments

For their help with field instrumentation, data collection/processing and presentation, the authors would like to acknowledge Charles A Harrison, Hydrology Technician, and Julie Arnold, Forestry Technician, both with the USDA Forest Service. The authors also are thankful to internal reviewers Dr. Peter Caldwell at the USDA Forest Service and Dr. Dariusz Młyński from the University of Agriculture in Krakow, Poland, for their valuable suggestions regarding the manuscript. Thanks also to Greta Langhenry and Maureen Stuart of the USDA Forest Service for their help with editing the manuscript. *The opinions presented in this article are those of the authors and should not be construed to represent any official USDA or U.S. Government determination or policy."*

Appendix A1

Equations to calculate direct runoff and its components (shallow subsurface saturated and overland surface runoff) in MSME model.
Streamside shallow subsurface saturated runoff (Q_{subs}) was calculated using following equations:

$$\mathrm{MSME}_{Qsubs} = \frac{(P - I_{a1})\cdot(P - I_{a1} + M)}{(P - I_{a1} + S_a)} \text{ if } P > I_{a1} \tag{A1}$$

$$I_{a1} = \alpha \bullet (S_a - M) \tag{A2}$$

$$\mathrm{MSME}_{Qsubs} = \text{if } P < I_{a1} \tag{A3}$$

$$M = \beta\cdot\frac{(P_5 - \lambda S_{a)}\cdot S_a}{(P_5 - \lambda S_{a)+}S_a} \text{ if } P_5 > \ \lambda S_a \tag{A4}$$

$$M = 0 \text{ for } \mathrm{P_5} < \lambda\mathrm{S_a} \tag{A5}$$

$$S_a = \alpha \bullet \left(\frac{25400}{CN} - 254\right) \tag{A6}$$

Watershedwide surface overland runoff (Q_{surf}) was calculated using equations:

$$\mathrm{MSME}_{Qsurf} = \frac{(P - I_{a2})\cdot(P - I_{a2})}{(P - I_{a2} + S_b)} \text{ if } P > I_{a1} + I_{a2} \tag{A7}$$

$$I_{a1} = (1 - \alpha) \bullet (S_b) \tag{A8}$$

$$\mathrm{MSME}_{Qsurf} = 0 \text{ if } P < I_{a1} + I_{a2} \tag{A9}$$

$$S_a = (1 - \alpha) \bullet \left(\frac{25400}{(100 - CN)} - 254\right) \tag{A10}$$

Total runoff Q_{tot} was calculated as the sum of overland and subsurface saturated runoff:

$$\mathrm{MSME}_{Qtot} = \mathrm{MSME}_{Qsurf} + \mathrm{MSME}_{Qsubs} \tag{A11}$$

where P is the sum of the precipitation during the event (mm), λ = a calibrated parameter that represents the initial abstraction coefficient, I_{a1} is the initial abstraction for shallow subsurface saturated runoff (mm), S_a is the maximum potential retention for the area where shallow subsurface saturated runoff occurs (mm), α is the coefficient for the proportion of the watershed area with saturated soil (this parameter is calibrated), I_{a2} is the initial abstraction for overland surface runoff (mm), S_b is the maximum potential retention for the area where overland runoff occurs (mm), M = antecedent soil moisture index (mm), CN is the CN parameter, MSME_{Qsubs} is the shallow subsurface saturated runoff (mm), and MSME_{Qsurf} is the overland surface runoff (mm).

Appendix B

References

Amatya, D.M., Trettin, C.C., 2010. Outflow Characteristics of a Naturally Drained Forested Watershed in Coastal South Carolina. Proceedings, 9th International Drainage Symposium at the XVIIth World Congress of the CIGR, Quebec, Canada.

Amatya, D. M., Trettin, C.C., 2021. Santee Experimental Forest, Watershed 80: streamflow, water chemistry, water table, and weather data. Fort Collins, CO: Forest Service Research Data Archive. https://doi.org/10.2737/RDS-2021-0043.

Amatya, D.M., Trettin, C.C., 2019. Long-term ecohydrologic monitoring: A case study from the Santee Experimental Forest, South Carolina. J. South Carolina Water Resour. 6 (1), 46–55.

Amatya, D.M., Skaggs, R.W., Gregory, J.D., 1996. Effects of controlled drainage on the hydrology of a drained pine plantation in the North Carolina coastal plains. J. Hydrol. 181, 211–232.

Amatya, D.M., Chescheir, G.M., Skaggs, R.W., 1998. Evaluation of Methods used in Estimating Outflow Rates in the Coastal Watersheds. In: Proc. of the 1998 ASCE Int'l Water Res. Engrg. Conf., Memphis (vol. 1), TN, Aug 3-7, 1998, pp. 850-855.

Amatya, D.M., Gregory, J.D., Skaggs, R.W., 2000. Effects of controlled drainage on storm event hydrology in a Loblolly pine plantation. J. Am. Water Resour. Assoc. 36 (1), 175–190.

Amatya, D.M., Callahan, T.J., Hansen, W.F., Trettin, C.C., Radecki-Pawlik, A., Meire, P., 2015. Turkey Creek – A Case Study of Ecohydrology and Integrated Watershed Management in the Low-Gradient Atlantic Coastal Plain, U.S.A. Journal of Water Resource and Protection, 2015, 7, 792-814.

Amatya, D.M., Fialkowski, M., Bitner, A., 2018. A numerical water table depth computing model for poorly drained soils. Wetlands. https://doi.org/10.1007/s13157-018-1069-7.

Amatya, D.M., Williams, T.M., Nettles, J.E., Skaggs, R.W., Trettin, C.C., 2019. Comparison of hydrology of two Atlantic coastal plain forests, USA. Trans. ASABE 62 (6), 1509–1529.

Amatya, D.M., Chescheir, G.M., Williams, T.M., Skaggs, R.W., Tian, S., 2020. Longterm water table dynamics of forested wetlands: drivers and their effects on wetland hydrology in the southeastern Atlantic coastal plain. Wetlands. 40, 65–79. https://doi.org/10.1007/s13157-019-01153-y.

Amatya, D.M., Tian, S., Marion, D., Caldwell, P., Laseter, S., Youssef, M.A., Grace, J.M., Chescheir, G.M., Panda, S., Ouyang, Y., Sun, G., Vose, J.M., 2021. Estimates of precipitation IDF curves and design discharges for road-crossing drainage structures: A case study in four small forested watersheds in the southeastern U.S. J. Hydrol. Eng. 26 (4), 05021004. https://doi.org/10.1061/(ASCE)HE.1943-5584.0002052.

Appling, A. P., M. C. Leon, and W. H. McDowell. 2015. Reducing bias and quantifying uncertainty in.

Appling, A.P., Leon, M.C., McDowell, W.H., 2015b. Reducing bias and quantifying uncertainty in watershed flux estimates: the R package loadflex. Ecosphere. 6 (12), 269. https://doi.org/10.1890/ES14-00517.1.

Baltas, E.A., Dervos, N.A., Mimikou, M.A., 2007. Technical Note: Determination of the SCS initial abstraction ratio in an experimental watershed in Greece. Hydrol. Earth Syst. Sci. 11, 1825–1829.

Bartlett, M.S., Parolari, A.J., McDonnell, J.J., Porporato, A., 2016. Beyond the SCS-CN method: A theoretical framework for spatially lumped rainfall-runoff response. Water Resour. Res. 52, 4608–4627. https://doi.org/10.1002/2015WR018439.

Bishop, K.H., Grip, H., O'Neill, A., 1990. The origins of acid runoff in a hillslope during storm events. J. Hydrol. 116, 35–61.

Blair, A.C., Sanger, D.M., White, D.L., Holland, A.F., Vandiver, C., Bowker, C., White, S., 2012. Quantifying and simulating stormwater runoff in watersheds. Hydrological Procesesses. 28 (3), 559–569. https://doi.org/10.1002/hyp.9616.

Blasone, R.-S., Vrugt, J.A., Madsen, H., Rosbjerg, D., Robinson, B.A., Zyvoloski, G.A., 2008. Generalized likelihood uncertainty estimation (GLUE) using adaptive Markov Chain Monte Carlo sampling. Adv. Water Resour. 31, 630–648.

Bonnel, M., 1993. Progress in the understanding of runoff generation dynamics in forests. J. Hydrol. 150, 217–275.

Bosch, D.D., Arnold, J.G., Allen, P.G., Lim, K.-J., Park, Y.S., 2017. Temporal variations in baseflow for the Little Riverexperimental watershed in South Georgia, USA. J. Hydrol.: Reg. Stud. 10, 110–121.

Callahan, T.J., Vulava, V.M., Passarello, M.C., Garrett, C.G., 2012. Estimating groundwater recharge in lowland watersheds. Hydrol. Process. 26, 2845–2855. https://doi.org/10.1002/hyp.8356.

Camporese, M., Paniconi, C., Putti, M., McDonnell, J.J., 2019. Fill and spill hillslope runoff representation with a Richards equation-based model. Water Resour. Res. 55, 8445–8462. https://doi.org/10.1029/2019WR025726.

Capece, J. C., Campbell, K. L., Baldwin, L. B., 1986. Estimation of runoff peak rates and volume from flatwoods watersheds. Gainesville, FL: University of Florida, Institute of Food and Agriculture Sciences.

Colquhoun, D.J., 1974. Cyclic surficial stratigraphic units of the Middle and Lower Coastal Plain, central South Carolina. Post-Miocene stratigraphy, central and southern Atlantic Coastal Plain. Utah State University Press, Logan, UT.

Corbin, J., H. Morgan, E. Patrohay, T. Williams, D. Amatya, C. Darnault. 2022. Hydrologic Modeling of Development Effect Scenarios on a Relatively Undisturbed Coastal Forest Watershed. Journal of South Carolina Water Resources, In Press.

Dai, Z., Trettin, C.C., Amatya, D.M., 2013. Effects of climate variability on forest hydrology and carbon sequestration on the Santee Experimental Forest in coastal South Carolina. Gen. Tech. Rep. SRS-GTR-172. Asheville, NC: USDA-Forest Service, Southern Research Station. 32 pp.

Dingman, S.L., 2002. Physical Hydrology. Prentice-Hall Inc, Upper Saddle River, NJ.

Dunne, T., Black, R.D., 1970. An experimental investigation of runoff production in permeable soils. Water Resour. Res. 6, 478–490.

Dunne, T., Moore, T.R., Taylor, C.H., 1975. Recognition and prediction of runoff-producing zones in humid regions. Hydrol. Sci. Bull. 20, 305–327.

Epps, T.H., Hitchcock, D.R., Jayakaran, A.D., Loflin, D.R., Williams, T.M., Amatya, D.M., 2013a. Characterization of storm flow dynamics of headwater streams in the South Carolina lower coastal plain. J. Am. Water Resour. Assoc. 49 (1), 76–89.

Epps, T.H., Hitchcock, D.R., Jayakaran, A.D., Loflin, D.R., Williams, T.M., Amatya, D.M., 2013b. Curve number derivation for watersheds draining two headwater streams in lower coastal plain South Carolina, USA. J. Am. Water Resour. Assoc. 49 (6), 1284–1295.

Eshleman, K., Pollard, J., O'Brien, A., 1994. Interactions between groundwater and surface water in a Virginia coastal plain watershed, 1. hydrological flowpaths. Hydrol. Process. 8, 389–410.

Famiglietti, J.S., Ryu, D., Berg, A.A., Rodell, M., Jackson, T.J., 2008. Field observations of soil moisture variability across scales. Water Resour. Res. 44, W01423. https://doi.org/10.1029/2006WR005804.

Fedelman, A.D., 2000. Hydrologic Modeling System HEC-HMS: Technical Reference Manual; US Army Corps of Engineers, Hydrologic Engineering Center: Davis. CA, USA.

Genereux, D.P., 2003. Comparison of methods for estimation of 50-year peak discharge from a small, rural watershed in North Carolina. Environ. Geol. 44 (1), 5358.

Grimaldi, S., Petroselli, A., Romano, N., 2013a. Green-Ampt Curve Number mixed procedure as an empirical tool for rainfall-runoff modelling in small and ungauged basins. Hydrol. Process. 27, 1253–1264.

Grimaldi, S., Petroselli, A., Romano, N., 2013b. Curve-Number/Green–Ampt mixed procedure for streamflow predictions in ungauged basins: Parameter sensitivity analysis. Hydrol. Process. 27, 1265–1275.

Haley, E.B., 2007. Field Measurements and Hydrologic Modeling of the Turkey Creek Watershed, South Carolina. M.Sc. thesis. College of Charleston, Charleston, South Carolina. 168 pp.

Harder, S., Amatya, D., Callahan, T., Trettin, C., Hakkila, J., 2007. A hydrologic budget of a first-order forested watershed, coastal South Carolina. J. Am. Water Resour. Assoc. 43 (3), 1–13.

Hawkins, R.H., Jiang, R., Woodward, D.E., Hjelmfelt, A.T., Van Mullem, J.A., Quan Q.D., 2002. Runoff Curve Number Method: Examination of the Initial Abstraction Ratio. In Proceedings of the Second Federal Interagency Hydrologic Modeling Conference, Las Vegas, Nevada, U.S. Geological Survey, Lakewood, Colorado, ASCE Publications.

Hayes, D.C., Young, R.L., 2006. Comparison of peak discharge and runoff characteristic estimates from the rational method to field observations for small basins in central Virginia. Scientific Investigations Report 2005-5254, U.S. Department of Interior, U. S. Geological Survey, Reston, VA 2006, 44 p.

HEC, 2006. Hydrologic modeling system; HEC-HMS, Users Manual. U.S. Army Corps of Engineers Hydrologic Engineering Center, Davis, CA USA.

Hewlett, J.D., 1982. Principles of Forest Hydrology. University of Georgia Press, Athens, GA, p. 192 p..

Hitchcock, D.R., Jayakaran, A.D., White, D.L., 2014. Green infrastructure in coastal landscapes: hydrological function, ecological design and sustainable land use guidance. J. South Carolina Water Resour. 1 (1), 32–38.

Hitchcock, D.R., Conner, W.H., Williams, T.M., Jayakaran, A.D., Esswein, S., Song, B., 2009. Monitoring sustainable development: the remote data acquisition network at Bannockburn Plantation. ASABE Paper 097369.

James, B.V., 2013. Time and Tide: Understanding the Water Dynamics in a Tidal Freshwater Forested Wetland. College of Charleston M.Sc. Thesis, Charleston, SC USA. 139 p.

Jin, X., Xu, C., Zhang, Q., Singh, V.P., 2010. Parameter and modeling uncertainty simulated by GLUE and a formal Bayesian method for a conceptual hydrological model. J. Hydrol. 383, 147–155.

Joo, J., Kjeldlsen, T., Kim, H.J., Lee, H., 2014. A comparison of two-event based flood models (ReFH-rainfall runoff model and HEC-HMS) at two Korean catchments. Bukil and Jeungpyeong, KSCE Journal of Civil Engineering. 18 (1), 330–343.

Juez, C., Peña-Angulo, D., Khorchani, M., Regues, D., Nadal-Romero, E., 2021. 20-years of hindsight into hydrological dynamics of a mountain forest catchment in the Central Spanish Pyrenees. Sci. Total Environ. 766, 142610 https://doi.org/10.1016/j.scitotenv.2020.142610.

Kannan, N., Santhi, C., Williams, J.R., Arnold, J.G., 2007. Development of a continuous soil moisture accounting procedure for curve number methodology and its behaviour with different evapotranspiration methods. Hydrologic Processes 22 (13), 2114–2121.

Kuichling, E., 1889. The relation between the rainfall and the discharge of sewers in populous districts. Transactions of the American Society of Civil Engineers 20 (1), 1–56.

La Torre Torres, I.B., 2008. Seasonal relationships between precipitation and streamflow patterns related to watershed characterization of two thirdorder coastal plain watersheds in South Carolina. M.Sc. thesis, College of Charleston, Charleston, SC.

La Torre Torres, I.B., Amatya, D.M., Sun, G., Callahan, T.J., 2011. Seasonal rainfall–runoff relationships in a lowland forested watershed in the southeastern USA. Hydrol. Process. 25 (13), 2032–2045.

Lockaby, G., Nagy, C., Vose, J.M., Ford, C.R., Sun, G., McNulty, S., Caldwell, P., Cohen, E., Myers, J.M., 2013. Forests and water. In: Wear, D.N.; Gries, J.G., eds. The Southern Forest Futures Project: technical report. Gen. Tech. Rep. SRS-178. Asheville, NC: U.S. Department of Agriculture Forest Service, Southern Research Station: 309-339.

Ma, C., Li, X., McCabe, M.F., 2020. Retrieval of High-Resolution Soil Moisture through Combination of Sentinel-1 and Sentinel-2 Data. Remote Sensing 12, 2303. https://doi.org/10.3390/rs12142303.

Martinez, G.F., Gupta, H.V., 2011. Hydrologic consistency as a basis for complexity of monthly water balance models for the continental United States. Water Resour. Res. 47, W12540. https://doi.org/10.1029/2011WR011229.

McDonnell, J.J., Owens, I.F., Stewart, M.K., 1991. A case study of shallow flow paths in a steep zero-order basin. J. Am. Water Resour. Assoc. 27, 679–685.

Menberu, M.W., Haghighi, A.T., Ronkanen, A.K., Kvarner, J., Klove, B., 2014. Runoff curve numbers for peat-dominated watersheds. J. Hydrol. Eng. https://doi.org/10.1061/(ASCE)HE.1943-5584.0001038.

Mishra, S.K., Singh, V.P., 2002. SCS-CN-based hydrologic simulation package. In: Singh, V.P., Frevert, D.K. (Eds.), Mathematical Models of Small Watershed Hydrology and Applications. Water Resources Publications, LLC, Highlands Ranch, pp. 391–464.

Młyński, D., Walega, A., Książek, L., Florek, J., Petroselli, A., 2020. Possibility of using selected rainfall-runoff models for determining the design hydrograph in mountainous catchments: A case study in Poland. Water. 12 (5), 1450. https://doi.org/10.3390/w12051450.

Moriasi, D.N., Arnold, J.G., Van Liew, M.W., Bingner, R.L., Harmel, R.D., Veith, T.L., 2007. Model evaluations guidelines forsystematic quantification of accuracy in watershed simulations. Trans. ASABE 50 (3), 885–900.

Morrison, A.E., 2016. Storm Event Analysis at Varying Watershed Scales: Turkey Creek, Santee Experimental Forest. South Carolina. College of Charleston M.Sc, Thesis, Charleston, SC USA, p. 334.

Nash, J.E., Sutcliffe, J.V., 1970. River flow forecasting through conceptual models: Part 1. A discussion of principles. J. Hydrol. 10 (3), 282–290.

NLCD, 2016. National Land Cover Database. https://www.mrlc.gov.

NWI, 2021. National Wetland Inventory. https://www.fws.gov/wetlands accessed on March 17, 2021.

O'Driscoll, M., Clinton, S., Jefferson, A., Manda, A., McMillan, S., 2010. Urbanization effects on watershed hydrology and in-stream processes in the southern United States. Water. 2, 605–648. https://doi.org/10.3390/w2030605.

Petroselli, A., 2020. A generalization of the EBA4SUB rainfall–runoff model considering surface and subsurface flow. Hydrol. Sci. J. 65 (14), 2390–2401. https://doi.org/10.1080/02626667.2020.1810856.

Ritter, A., Muñoz-Carpena, R., 2013. Performance evaluation of hydrological models: Statistical significance for reducing subjectivity in goodness-of-fit assessments. J. Hydrol. 480, 33–45. https://doi.org/10.1016/j.jhydrol.2012.12.004.

Rossman, L.A., Huber, W.C., 2016. Storm Water Management Model Reference Manual Volume I—Hydrology (Revised); US EPA Office of Research and Development, Washington, DC, EPA/600/R-15/162A, 2015.

Seibert, J., Bishop, K., Nyberg, L., Rodhe, A., 2011. Water storage in a till catchment. I: Distributed modeling and relationship to runoff. Hydrol. Process. 25, 3937–3949.

Sheridan, J.M., Merkel, W.H., Bosch, D.D., 2002. Peak rate factors for flatland watersheds. ASABE Appl. Eng. Agric.. 18 (1), 65–69.

Skaggs, R.W., Tian, S. Chescheir, G.M. Amatya, D.M. Youssef, M.A., 2016. Forest Drainage. In Ch. 14: Forest Hydrology: Processes, Management, and Applications, D. M. Amatya, T.M. Williams, L. Bren, and C. de Jong (Editors), CABI Publishers, UK, pp: 124-140.

Slattery, M.C., Gares, P.A., Phillips, J.D., 2006. Multiple modes of storm runoff generation in a North Carolina coastal plain watershed. Hydrologic Processes 20 (14), 2953–2969. https://doi.org/10.1002/hyp.6144.

Soulis K.X., Valiantzas, J.D. 2012. SCS-CN parameter determination using rainfall-runoff data in heterogeneous watersheds – the two-CN system approach. Hydrology and Earth System Sciences 16, 1001-101.

Swindel, B., Lassiter, C., Riekerk, H., 1983. Effects of different harvesting and site preparation operations on the peak flows of streams in *Pinus elliottii* flatwoods forests. For. Ecol. Manage. 5, 77–86.

Tedela, N.H., McCutcheon, S.C., Rasmussen, T.C., et al., 2012. Runoff curve numbers for 10 small forested watersheds in the mountains of the Eastern United States. J. Hydrol. Eng. 17 (11), 1188–1198.

USDA, 2004. Estimation of direct runoff from storm rainfall. Chapter 10, part 630. National Engineering Handbook, United States Department of Agriculture (USDA) Soil Conservation Service, Washington, USA. pp 1-22.

USDA, 1986. Urban hydrology for small watersheds. Tech. Release No. 55. Washington, DC: United States Department of Agriculture (USDA) Soil Conservation Service, Washington, USA.

USDA, 1980. Soil Survey of Georgetown County South Carolina. Soil Conservation Service, Washington, D.C.

Verma, S., Singh, P.K., Mishra, S.K., Singh, V.P., Singh, V., Singh, A., 2020. Activation soil moisture accounting (ASMA) for runoff estimation using soil conservation service curve number (SCS-CN) method. J. Hydrol. 589, 125114 https://doi.org/10.1016/j.jhydrol.2020.125114.

Walega, A., Książek, L., 2016. Influence of Rainfall Data on the Uncertainty of Flood Simulation. Soil Water Res. 11 (4), 277–284. https://doi.org/10.17221/156/2015-SWR.

Walega, A., Cupak, A., Amatya, D.M. Drożdżal, E., 2017. Comparison of direct outflow calculated by different methods for mountainous and highland catchments in Upper Vistula basin, Poland and lowland catchment in South Carolina, USA. Acta Sci. Pol., Formatio Circumiectus. 16(1), 187–207. DOI: 10.15576/ASP.FC/2017.16.1.187.

Walega, A., Amatya, D.M., 2020. Modification of the SME-CN method for predicting event runoff and peak discharge from a drained forest watershed on the North Carolina atlantic coastal plain. Trans. ASABE 63 (2). https://doi.org/10.13031/trans.13838.

Walega, A., Amatya, D.M., Caldwell, P., Marion, D., Panda, S., 2020. Assessment of storm direct outflow and peak flow rates using improved SCS-CN models for selected forested watersheds in the southeastern United States. J. Hydrol. – Regional Stud. 27 https://doi.org/10.1016/j.ejrh.2019.100645.

Walker, S.E., Banasik, K., Northcott, W.J., Jiang, N., Yuan, Y., Mirchell, J.K., 2001. Application of the SCS Curve Number Method to Mildly-Sloped Watersheds. Southern Cooperative Series Bulletin.

Wilcox, B.P., Dean, D.D., Jacob, J.S., Sipocz, A., 2011. Evidence of Surface Connectivity for Texas Gulf Coast Depressional Wetlands. Wetlands 2011 (31), 451–458.

Williams, T.M. Amatya, D.M., 2016. Coastal Plain Soils and Geomorphology: A key to Understanding Forest Hydrology. *In:* Headwaters to estuaries: advances in watershed science and management (pp 14-21), Proc. of the 5th Interagency Conference on Research in the Watersheds. Editors: Stringer, C.E.; Krauss, K.W.; Latimer, J.S, e-Gen. Tech. Rep. SRS-211. Asheville, NC: U.S. Department of Agriculture Forest Service, Southern Research Station. Station, http://www.srs.fs.usda.gov/pubs/50141#sthash.WM9AViYu.dpuf.

Williams, T.M. 1979. Implications of hydrologic response to the practice of forestry on coastal forests. pp 92- 102 In Smith, W.H. (ed.) Proceedings: Forest Practice and Water. 1979 Annual Meeting, Florida Section, Society of American Foresters (SAF).

Williams, T.M. 2007. Evidence of runoff production mechanisms in low gradient coastal forested watersheds. ASAE/CSAE Meeting Paper No. 072228. St. Joseph, MI, CD-ROM.

Woodward D.E., Hawkins R.H., Jiang R., Hjelmfelt A.T. Jr., Van Mullem J.A., Quan D.Q., 2003. Runoff Curve Number Method: Examination of the Initial Abstraction Ratio. World Water & Environ. Resour. Congress and Related Symposia, EWRI, ASCE, 23–26 June, 2003, Philadelphia, Pennsylvania, USA.

Xiong, L.H., Wan, M., Wei, X.J., 2009. Indices for assessing the prediction bounds of hydrological models and application by generalized likelihood uncertainty estimation. Hydrol. Sci. J. 54, 852–871.

Younger, P.L., 2006. In: Groundwater in the Environment. Wiley-Blackwell, Inc., p. 332. ISBN-13: 978-1405121439.

Zhai, Y., Wang, C., Chen, G., Wang, C., Li, X., Liu, Y., 2020. Field-based analysis of runoff generation processes in humid lowlands of the Taihu Basin, China. Water 12, 1216. https://doi.org/10.3390/w12041216.